

HIGH-THROUGHPUT COMBINATORIAL STUDY
OF LOCAL MECHANICAL PROPERTIES IN
THIN FILM COMPOSITION SPREADS

A Dissertation

Presented to the Faculty of the Graduate School
of Cornell University

in Partial Fulfillment of the Requirements for the Degree of
Doctor of Philosophy

by

Noble C. Woo

January 2012

© 2012 Noble C. Woo

ALL RIGHTS RESERVED

HIGH-THROUGHPUT COMBINATORIAL STUDY OF LOCAL MECHANICAL PROPERTIES IN THIN FILM COMPOSITION SPREADS

Noble C. Woo, Ph. D.

Cornell University 2012

Mechanical properties such as residual stress and magnetically induced strain such as magnetostriction in thin film can be measured using singly clamped cantilevers. By having a freshly deposited film on a cantilever, residual stress can be measured by simply determining curvature of the bending cantilever beam. Likewise, the coefficient of magnetostriction can also be determined by measuring curvature of a unimorph consisted of a magnetic layer and a non-magnetic cantilever under the application of magnetic field. Such sensitive experiment can offer quantitative evaluation of the material property being investigated. By applying the curvature measurement technique to combinatorial materials science, a high-precision, quantitative instrument has been developed for measuring these properties on thin film composition spreads with unprecedented composition resolution. In this approach, the thin film composition spread is deposited on a dense array of MEMS-based prefabricated cantilevers. The curvature of the cantilevers is interrogated using an optical curvature measurement approach that is fast and precise. This system allows high-throughput local measurements of stresses in composition-spread samples. By automating the data acquisition with precise stage movements, it takes approximately 2 hours to measure 2500 cantilever curvatures, including preparation time required for registration and alignment of cantilevers, and calibration of detector sensitivity. The Fe–Ni–Al composition system is used as a case study to validate this approach. Residual stresses are measured at 1-millimeter intervals on the Fe–Ni–Al composition spread film. Since the composition spreads typically have a composition gradient on the order of 1 atomic % per millimeter, this technique enables investigation

of thin film mechanical properties with 1 atomic % resolution. This measurement system has a relatively high dynamic range and high sensitivity, which can enable high-throughput investigation of a wide range of other mechanical properties, such as conventional and ferromagnetic shape-memory effects, thermal expansion coefficients, and magnetostrictive properties. To demonstrate the high sensitivity and versatility of this system, thin film magnetostriction coefficients of NiFe alloy are measured to strains as small as 0.1 parts per million. With improvement in sensitivity, this approach can also be used in measuring surface stress of ultrathin films.

BIOGRAPHICAL SKETCH

Noble Chark-Fu Woo was born in the city of Tavoy (Dawei) in a Southeast Asian country of Burma (Myanmar) on May 22, 1977. Having immigrated to the US at the age of 16, he finished high school at 20. He attended UC San Diego from 1997 to 2001 where he obtained a bachelor of science in Physics. He spent one year at Sandia National Laboratories in Livermore, CA as a technical staff member prior to starting his graduate studies at Cornell University in August 2002. He obtained a master of science in Chemistry and Chemical Biology in January 2005. Although he defended his dissertation on September 11, 2007, he completed his doctor of philosophy in Chemistry and Chemical Biology at Cornell University in January 2012.

ACKNOWLEDGEMENTS

First and foremost, I would like to thank my advisor, Bruce van Dover, for his support and guidance over the “long” years. It was Bruce who first suggested that I took on a preliminary project, which he thought should not take more than six months. After designing and building a robust measurement system that met the early objectives of the project, two and a half years had already gone by, forcing me to start writing up for the dissertation. I would like to gratefully thank Professor Melissa Hines who had always supported me, even before I arrived to Ithaca. She was responsible for pulling my application from the applied physics department to accept me into the chemistry department. She also guided me to work with Bruce and supported me with the GAANN scholarship in my last year of studies. I would also like to thank Professor Francis DiSalvo for serving on my dissertation committee and for being honest and straightforward with my progress during the studies. I must also thank Professor John Marohn for his cheerfulness and full optimism that infected me every time I had a chance to converse. I would also like to thank Professor Ralph Spolenak of ETH Zurich for hosting me during my short stay in Switzerland in 2006. This opened my eyes about life and the existence of research opportunities outside the States, while exposing me to the delicate balance of work and life of Europeans. Consequently, I went on to work with Ralph at ETH as a postdoctoral fellow afterward.

During my studies, I spent most of my time either in the Cornell Nanoscale Facility cleanroom or in our Duffield/Bard labs. I would like to thank all the CNF staff because without their knowledge and skills, I would not be able to carry out microfabrications required for my

dissertation work. I was grateful for my colleagues - Jon Petrie, Sara Barron, John Gregoire, Karen Downey, Mark Prochaska and Steve Kirby - with whom I spent much of the time either talking about sputter deposition or drudge report. Raiders beat chargers every single time, Jon. I would also like to thank my colleagues from ETH Zurich with whom I had the pleasure of working and helped make my time enjoyable in Switzerland.

Ithaca, however gorgeous it was, was not really known for nice weather for the majority of the year. Thanks to the two things beside my graduate studies that kept me from packing my bags to leave Ithaca in the cold gloomy days: soccer and social dancing. From my very first summer in Ithaca, I was fortunate to enjoy playing soccer with many of my chemistry classmates. We even formed two teams named - Entropy and Enthalpy – what a bunch of nerds! Needless to say, that pleasure, thanks to my teammates, continued for every week until I left Ithaca. Social life at Cornell could be really dreadful - with full of brains but not so many beauties - which forced me to venture outside my department to meet my future wife Benedetta Bartali with whom I had a wonderful daughter, Gemma.

Lastly I would like to thank my family. Without my brave grandma Chu who learned English to pass the citizenship interview at her young age of 65, I would have never set foot in the States, let alone getting a PhD. I want to thank my younger brothers and sister, Robyn, Allen, Ronnie and Richie for taking care of mom and dad while I was away at Cornell and allowing your big brother to achieve something meaningful in life. Of course without my mom and dad with their purest heart and love and support, I would have never begun my studies.

Table of Contents

1	Introduction	1
1.1	Thin Film Materials	2
1.2	Residual Stress	9
1.3	Magnetostriction	11
1.4	Combinatorial Materials Science	14
1.5	High-Throughput Characterization	16
2	General Description of Experimental Techniques for High-Throughput Combinatorial Studies	18
2.1	Introduction	19
2.2	Sample Preparation for Combinatorial Synthesis	20
2.2.1	Choosing the Substrate Platform	21
2.2.2	Designing the Cantilever Array Fabrication	23
2.3	Microfabrication Process Flow	26
2.3.1	Designing the Photolithographic Mask for Pattern Transfer	26
2.3.2	Mask Generation of Cantilever Array Pattern	26
2.3.3	Photolithography - The Pattern Transfer from Mask to Substrate Platform	28
2.3.4	Low Pressure Chemical Vapor Deposition of Silicon Nitride (Si_3N_4)	29
2.3.5	Reactive Ion Etching	30
2.3.6	Wet Etching – KOH	30
2.3.7	Critical Point Drying	32
2.4	Sputter Deposition of Composition Spreads	33
2.4.1	Sputter Deposition System	34
2.4.2	Sputter Deposition Profile	37
2.5	Thin Film Characterization	38
2.5.1	Electron Microprobe – EDX	39
2.5.2	X-ray Diffraction – XRD	39
2.5.3	Nanoindentation	39
2.5.4	Scanning Electron & Optical Microscopy	40
2.6	Instrumentation for Curvature Measurement	43
2.6.1	LabView Integration – Virtual Control Interface	46
2.6.2	Optical Measurement Setup	47
2.6.2.1	Position Sensitive Detector – PSD	47

2.6.2.2	Objective Focusing Lens	48
2.6.2.3	Beam Splitter	48
2.6.3	Helmholtz Coils Control – (for Magnetostriction Measurement)	49
2.6.4	Integration of Precision Stage Movement & Scanning Algorithms	51
2.6.4.1	Calibration to Wafer Rotations	54
2.6.4.2	Scanning Algorithms	56
2.6.4.3	Scanning Efficiency	57
3	Residual Stress Measurements in Thin Film Composition Spreads	60
3.1	Introduction	61
3.2	Experimental Details	61
3.2.1	Sample Production for Residual Stress Measurements	62
3.2.2	Experimental Setup for Residual Stress Measurements	63
3.3	Residual Stress Measurement & Analysis	66
3.4	Discussion of Experimental Artifacts	72
3.4.1	Optical Measurement Setup	72
3.4.2	Stability of Measurements for The Entire Cantilever Array	74
3.4.3	Influence of Environment	75
4	Magnetostriction Measurement	76
4.1	Introduction	77
4.2	Experimental Details	79
4.2.1	Sample Preparation	79
4.2.2	Measurement Setup	80
4.3	Calculation of Magnetostriction	82
4.4	Reliability of Magnetostriction Measurement	85
5	Conclusions	87
5.1	Summary & Future Prospects	88

CHAPTER 1
INTRODUCTION

1.1 THIN FILM MATERIALS

The term “thin film” commonly refers to a thin layer of material constructed by various deposition processes, including chemical vapor deposition, physical vapor deposition and solution-based electrodeposition. Certain atom-by-atom deposition techniques allow fabrication of materials at the nanoscale, down to a few layers of atoms using processes such as atomic layer deposition and molecular beam epitaxy, and up to a larger thickness of several micrometers using processes such as electrodeposition and physical vapor deposition. Films are usually deposited onto a rigid substrate, which can then be removed to achieve freestanding films, which are suitable for utilization as highly sensitive membranes for various electronic, acoustic and optosonic applications [1-2]. Alternately, films on a substrate platform can be lithographically patterned to achieve the desired structural properties and electronic functionalities, such as integrated circuits (IC) and micro-electro-mechanical systems (MEMS). Deposition of materials with dissimilar properties or elemental compositions is often exploited to obtain multilayered composites that can potentially possess highly improved mechanical, structural, electronic and magnetic properties, which are otherwise unobtainable. These types of thin films are ubiquitous in our current technologies that play a very important role in improving our daily life, in applied science and technology, and national security. Advances in microelectronics and thin-film coatings are primarily based on engineering and manipulation of such thin films into the desired layers, components and devices. Examples of industrial applications include protective coatings for wear and tear purposes, microelectronics using multilayer components of metal and insulating films, semiconductor films used in optoelectronics and photovoltaics, multilayer dielectric films used as optical coatings, and magnetic storage devices based on thin anti-ferro/ferromagnetic multilayer films. For national security, a broad range of mission-critical military programs extensively employ various high-temperature coatings, microelectronic sensors, actuators and MEMS-based devices [1-2]. Given the soaring need for these materials in its most advanced and functional form, there is a commensurate effort to elaborate the

understanding of the intrinsic nature and behavior of these thin films in order to better control and fabricate exceedingly complex multilayer film structures.

Although thin film materials have a wide variety of useful properties such as electromechanical, optical and magnetic properties, many of these properties are noticeably different from those of their bulk counterparts. This necessitates the need for an extensive investigation based on its physical form, which creates particularly interesting areas of research in which the bulk and its various thin film counterpart offer a wide range of differing intricate physics and complex chemistry that govern their distinctive behaviors. With the increasingly interdisciplinary nature of applications, new demands for film characterization and property measurements are arising. This necessity has led to the development of an impressive array of commercially available analytical instruments; such instruments are ubiquitous in the thin-film community (Fig 1.1). Depending on the type of property investigated, it is often just a matter of modifying the existing techniques to suit thin film applications. Examples of these techniques include mechanical characterization techniques such as stress measurements suitable for thin films, and magnetic characterization techniques such as magnetostriction measurements.

One important use of thin films in our everyday life can be seen in metallurgical and protective coatings (Fig 1.2). These thin-film coatings can function as reflective, diffractive, decorative, conductive, corrosive, erosive, moisture and electrical protective, wear resistive and adhesive materials, just to name a few properties. In some cases, especially when rare and precious materials and metals are involved, a thin film is used for its surface property in order to save material. Examples can be seen in electroplating of gold thin films for decorative purposes and for superior electrical conductivity in home entertainment cable wires. In these applications, as thin a film as possible is desired for obvious economic reasons.

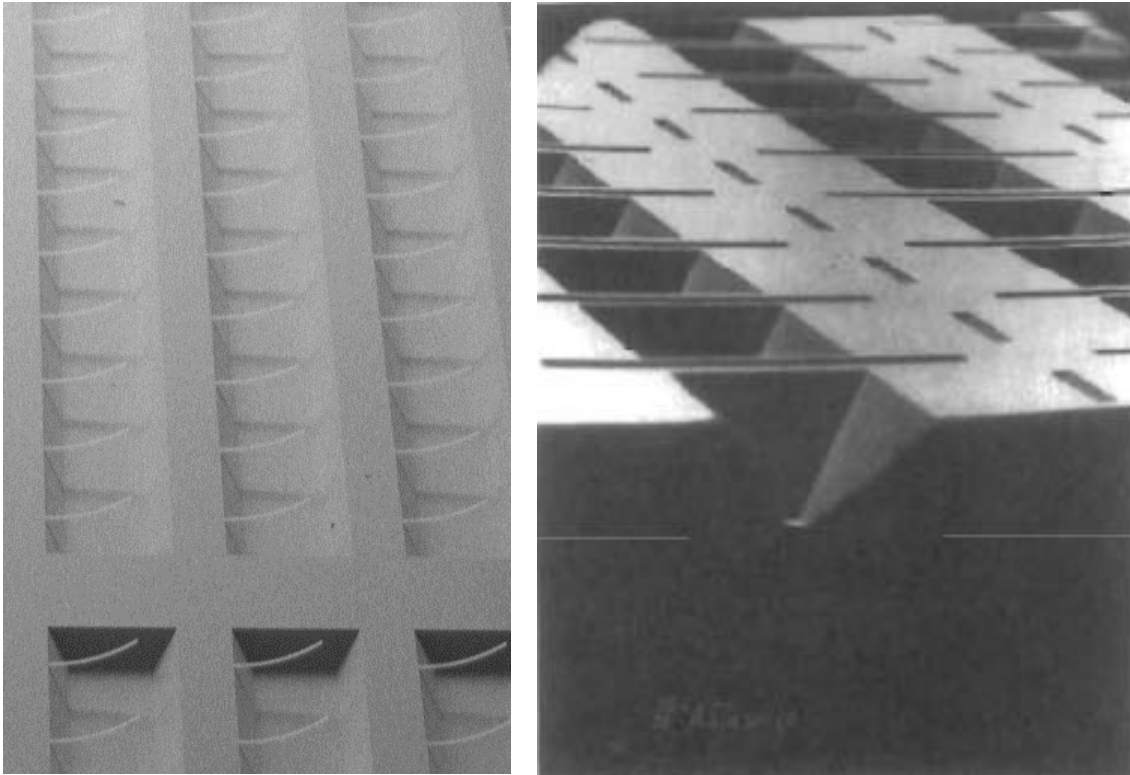


Figure 1.1: (Left) SEM micrograph of micro-cantilever arrays exhibiting as-deposited stress. (Right) SEM micrograph of optical micro-assembly. (AT&T Bell Laboratories).

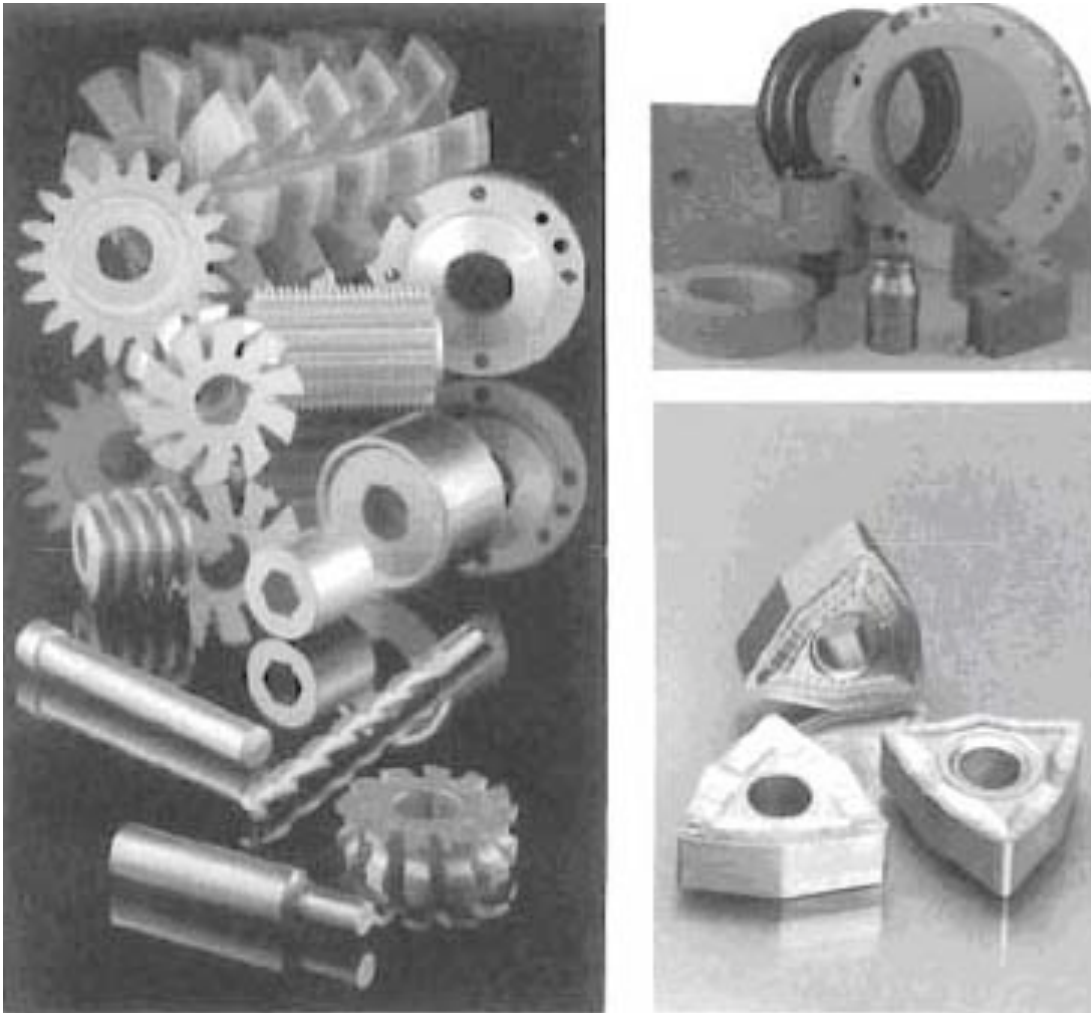


Figure 1.2: (Left) Assorted cutting and forming tools coated with TiN and multilayer coatings. (Multi-Arc Scientific Coatings). (Top right) HSS forming and sheet metal dies coated with TiN and TiC. (Ti Coating Inc.) (Lower right) multilayer coated cutting tool inserts. (S. Wertheimer, ISCAR Ltd.)

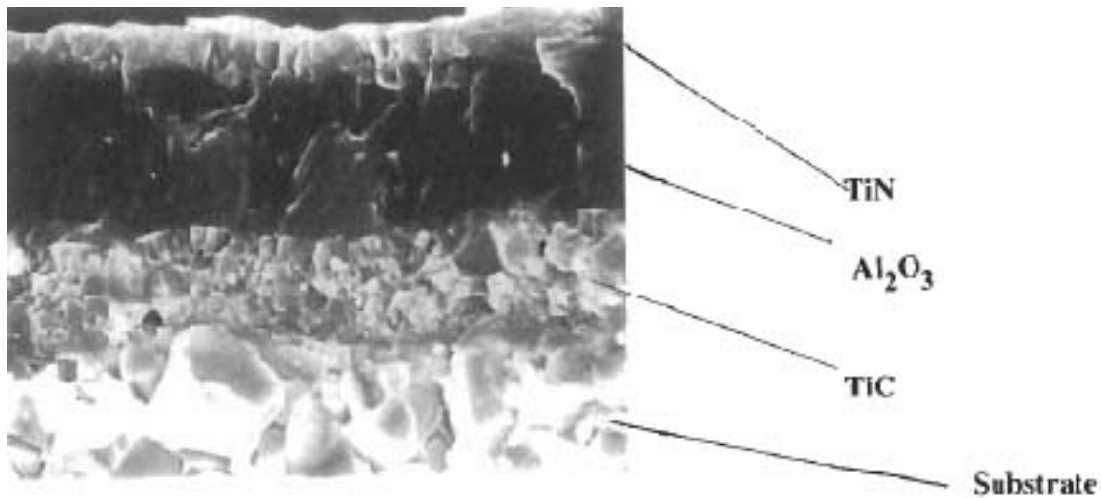


Figure 1.3: SEM images of CVD multilayer coatings for cutting tool inserts made from Carbide substrate with TiC-Al₂O₃-TiN multilayer-stack. (S. Wertheimer, ISCAR Ltd.)

On the other hand, a thin film used for protective purposes may need to be as thick as possible to offer the maximum wear and tear protection (Fig 1.3). An example is rust-resistant paint, which requires a thick-film deposition technique (i.e. spray-painting) but a very thick film is desired to prolong the lifetime. In such scenario, the stress in the deposited film and adhesion properties are the determination factors in the maximum obtainable thickness of films produced. Delamination and cracking in the coatings are the most common ways to relax the stresses for the thicker-than-desired films. To avoid these failures, it is very important to understand and control the stress each particular material can exhibit on particular substrate or host platform. Hence quantitative measurement of stress is crucial to prevent the equipment from damage.

Another important use of thin films in microelectronics industry is the utilization of magnetic thin-films in storage and memory devices (Fig 1.4). The potential interests in the application of magnetic thin films arose primarily because of their capability as fast-switching components that can act as computer memory elements. This particular property has triggered intense research and development efforts in the microelectronics industries that eventually led to

the development of devices based on magnetic devices such as high-capacity hard disks and magnetic random access memories (MRAM). The current challenge is the continual improvement of these magnetic devices to ensure better performance, lower power consumption, while offering larger capacity. Such advancement mainly depends on miniaturizing devices based on increasingly thinner films to create components with increasingly smaller volume to surface ratio. With each successive generation of miniaturization an increasing level of mechanical stability is required to control stresses that are created from binding of dissimilar materials. Understanding and controlling stresses that arise intrinsically and during operation of these new devices are crucial in designing and engineering of the next generation magnetic devices.

Intrinsic stress, usually present in “as-deposited” thin films as residual stress, is inherent in all thin films. It typically arises from the lattice mismatch between the thin film that is deposited and the host substrate. For multilayer films, lattice mismatch due to the difference in lattice spacing of the two adjacent films is one of many sources of stress that include incorporated voids that can lead to tensile stress and interstitials that lead to compressive stress. Understanding and controlling this form of stress is one of the foremost concerns in designing thin film devices. In contrast, the extrinsic stresses arise when excited by an external force, i.e., during operation of thin film devices. One example of an extrinsic stress is the magnetostrictive stress that is unique to ferromagnetic materials during magnetization. Understanding and controlling this magnetically induced stress in magnetic storage devices during operation is important because this unwanted phenomenon represents an important factor for device failure [3].

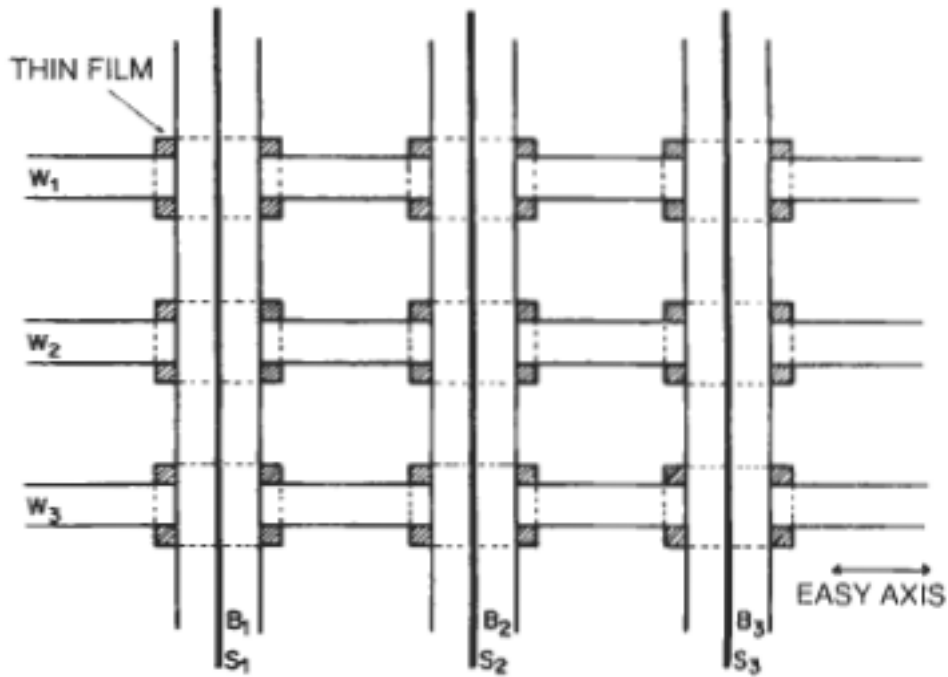


Figure 1.4: A magnetic film based memory (MRAM) plan with word lines W_1 , W_2 , and W_3 , bit lines B_1 , B_2 , and B_3 and Sense lines S_1 , S_2 , and S_3 . (McGraw-Hill, Inc.)

Despite advances in thin-film measurement techniques, determination of the residual stress and other mechanical properties in the films is still challenging. In this dissertation, I describe the development of a high-throughput measurement system capable of evaluating residual stress and magnetostriction properties of thin films with high spatial resolution. Using a micro-electromechanical systems (MEMS) fabricated cantilever in conjunction with laser-based optical-deflection measurements, the stress of a thin film is determined by measuring the curvature of a bilayer. If a thin film has spatially varying compositions, as in the case of composition spread samples produced by co-sputter deposition, thin film stress can be measured as a function of material composition. High-throughput analysis is enabled by rapid, automated measurements of individual cantilevers with distinct compositions.

1.2 RESIDUAL STRESS

Residual stress refers to the internal stress present in a material system with unconstrained boundaries. The existence of residual stress in thin films deposited on substrates has been observed since in the early 19th century. Although the effects of stress on film properties were recognized as important issues surrounding thin film utilization even then, it was only recently that the need to quantitatively determine and characterize this stress has been considered critical. Improperly controlled film stress can lead to film delamination, cracking, and buckling. If the film is used as a structural component, these modes of film relaxation degrade function; extensive deterioration will lead to device failure. Reliability concerns have prompted a thorough examination of stress effects on overall device function. The analysis of failure modes related to stress requires quantitative determination of as-deposited stress in the films. Even more challenging is the fact that as device dimensions shrink to accommodate faster performance or larger memory capacity, more diligent understanding and controlling of these stresses will be required. Precise measurement of film stress has become significant as smaller and smaller stresses may play a vital role in device properties with decreasing structural dimensions. These factors motivate the development of techniques to measure residual stress.

Over the last few decades, quantitative and qualitative methods have been developed for measuring stress. An important distinction is made between destructive and non-destructive techniques to determine such stress. Destructive techniques involve peeling off films from the host substrate and analyzing the resulting released films. These techniques may or may not accurately measure the stress in the bonded film. As a result, these techniques have become obsolete with the advent of non-destructive measurement methods. Only non-destructive techniques and measurement systems of thin film stress are discussed in this study.

Commercially available stress measurement systems such as kSA MOS (k-Space Inc, USA) typically determine the average stress over an entire ~ 3-inch substrate by measuring the overall surface curvature. This technique is well-suited to stress measurements in single-composition uniform films. Some advanced systems can also determine stresses of multi-layered

films [4]. However, these instruments cannot measure local stresses, as would be needed to characterize a non-uniform (e.g., combinatorial) film. For such films with a composition gradient, it would be ideal to have surface curvature measurement system capable of measuring a small enough region that the composition can be considered essentially uniform over the region.

X-ray diffraction (XRD) techniques have been used to measure lattice strains with extremely fine stress resolution [1-2]. This technique, however, demands either access to a synchrotron or else a very long integration time to acquire adequate counting statistics with in-house XRD systems. One stringent requirement for this technique is that the films must be highly crystalline so that the diffraction peaks can be precisely located. Along with *a priori* identification of the phases present in the film, knowledge of the indices of the diffracting planes is also required to infer the lattice constants of the film material from the measured *d*-spacings. X-ray diffraction is therefore not suitable for routine mapping of stress in inhomogeneous thin films.

This dissertation describes the development of technique to measure local stresses in thin film co-deposited composition spreads samples with an unprecedented (~ 1 atomic %) composition resolution and with ~ 0.1 MPa differential stress resolution. The system is based on measurement of the surface curvature of a dense array of microfabricated cantilevers. The small cantilevers needed to achieve the desired lateral spatial resolution have inherently less sensitivity than is achieved in curvature measurement employing large, centimeter-scale substrates. However our $1\text{-}\mu\text{m}$ thick cantilevers, being thin, have a very high compliance, which results in better sensitivity of measurement. Our system exhibits a stress sensitivity equivalent to a 10 kilometer radius of curvature on a 1-centimeter substrate, which translate to 70-80 kilometer radius for a full 3-inch $385\text{-}\mu\text{m}$ thick Si wafer, comparable to the state of the art measurement sensitivity [5-7].

1.3 MAGNETOSTRICTION

Magnetostriction is a property of ferromagnetic materials in which strain develops in response to an external magnetic field by lengthening or contraction (Fig 1.5). Depending on the orientation of the magnetic dipole moment with respect to the crystal lattice, elongation or shortening of the sample can be observed, generally along the axis of the applied magnetic field. This physical change is known as magnetostriction and its coefficient, λ , is defined as the net change Δl divided by initial length l . Typically λ values are on the orders of tens of parts per million (ppm) for transition-metal-based alloys, such as those containing iron (Fe), nickel (Ni), and cobalt (Co). The highest known λ values belong to alloys containing rare-earth metals, such as terbium (Tb).

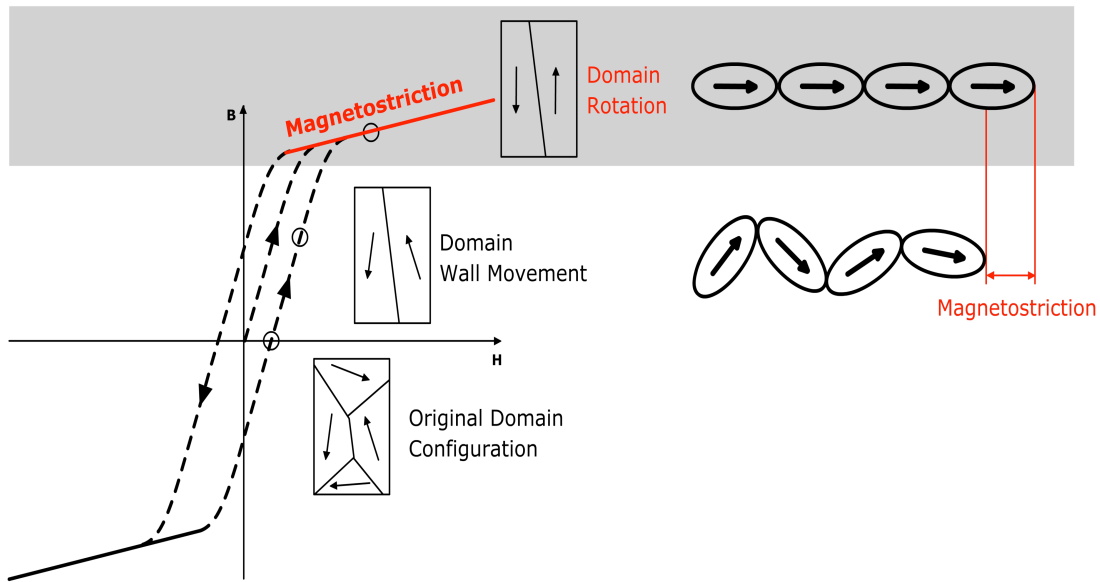


Figure 1.5: A depiction of how domains of a magnetic material react under an applied magnetic field (left) and an illustration of how domain rotation can cause materials expansion (right).

Thin film magnetostrictive materials have found use in actuation and sensing devices. One of the benefits of these materials over piezoelectric materials, which are the key components in conventional devices, is that they can operate at relatively higher frequencies since the magnetostriction effect is only limited by ferromagnetic resonance frequencies [8-10]. Since the principle of operation is through magnetic actuation, these devices can be remotely triggered and more importantly, they will have less performance degradation over time because it is non-contact operation, compared to mechanical means of actuation. The low processing temperatures required during device fabrication ($< 400^{\circ}\text{C}$) are also advantageous, as these temperatures are within typical thermal budgets.

Magnetostrictive actuators are typically constructed with giant magnetostrictive materials, such as Tb-based alloys. The Tb-based alloys have saturation magnetostriction coefficients exceeding 2,000 ppm [8]; however these changes can only be achieved in large magnetic fields (> 10 kOe). In comparison, Earth's magnetic field is a mere 0.5 Oe. Recent advances in magnetic research have led to development of new magnetostrictive materials with high magnetostrictive susceptibility, which is defined to be the magnetostriction per magnetic field, $d\lambda/dH$. These newly developed materials exhibit dimension increases of 470 ppm in magnetic fields as low as 100 Oe [11].

Sensing devices can be designed to use the inverse property of magnetostriction. Physical deformation of magnetostrictive materials, which depends on the extent of the stress, can generate a change in the magnetization directly proportional to the magnitude of the stress exerted. Magnetostrictive sensors may be used to detect changes in force, temperature, pressure, or magnetic field in a variety of applications. For example, magnetically-transduced surface acoustic wave devices employ magnetostrictive materials both as generators of high-frequency acoustic waves and detectors of these waves [12]. These devices have the potential to be used as versatile biological and chemical sensors.

Scientists and engineers have long been interested in characterizing magnetostrictive properties in both bulk and thin film forms. In bulk materials the magnetostriction coefficient

λ is straightforwardly measured by conventional strain gauges; data have been collected for many common elements and alloys [8]. The determination of magnetostriction coefficients in thin films is more challenging, as the size of the films precludes the use of strain gauges. In practice, magnetic thin films are typically deposited onto a substrate to form a bi-layer of magnetic film and nonmagnetic substrate. In these applications, the magnetic films are usually much thinner than their respective substrates. A more useful way to determine magnetostriction is to make a precise determination of the curvature of the bi-layer strip as a function of applied magnetic field.

Further improvements to thin-film magnetostrictive devices require investigations into unexplored materials compositions and their microstructures. The main limitation in the exploration of magnetostrictive materials is the inefficiency in current testing methods, as new compositions have to be constructed and evaluated individually. Since processing conditions such as deposition rate, gas pressure, and background vacuum level affect the property of thin films greatly, one-off experiments can exhibit uncontrolled variations that strongly affect the magnetostriction property of the sample. Therefore it is desirable that process conditions are well controlled so that only one parameter can be varied from one sample to another, while holding all other variables constant. For all these reasons, the combinatorial approach is highly advantageous for enabling materials synthesis of many samples (compositions) in a single experiment, reducing inconsistency across the sample space.

As in the residual stress measurements, the co-deposited composition spread technique is one way to synthesize a wide range of materials in a single experiment. However, its application to magnetostriction measurements of thin films has been limited. To take advantage of the composition spreads, a key challenge is to develop techniques capable of characterizing physical properties in a rapid and automated fashion. The use of micromachined cantilevers as a substrate platform for sputtered composition spreads has been suggested as a convenient method of probing physical properties [13]. Since different material compositions coat the top surface of each cantilever, each bilayer responds differently under external stresses, such as a magnetic

field or temperature gradient. Several investigators have used this technique to map the transition temperatures of ferromagnetic shape-memory alloys for ternary composition spreads [12-13]. However, their measurement methods have shown poor compositional resolution, approximately 3 atomic %, and are only able to discern large physical changes due to the use of relatively large size of cantilevers (3 mm x 15 mm). Although the composition resolution of their systems is novel, it is not nearly enough to resolve highly composition-sensitive properties, such as shape memory alloy with composition close to Ni₅₀Ti₅₀, where less than 1 atomic % change from the 50-50 ratio would disable the shape memory effect [12]. We have developed a high-throughput testing system for thin film magnetostriction measurements that utilizes ternary composition spreads sputtered onto micromachined cantilevers array. Small cantilevers and a highly sensitive optical measurement system allow this system to explore large composition ranges at small composition intervals (approximately 1 atomic percent change per cantilever), as well as enable magnetostriction measurements with a resolution of approximately 1 ppm.

1.4 COMBINATORIAL MATERIALS SCIENCE

For the past quarter of a century combinatorial materials science has served as a method for “high-throughput” synthesis and characterization of materials [13-16]. By eliminating inconsistencies often observed in conventional one-off experiments, the combinatorial approach also offers a unique method for detecting subtle trends in properties as a function of composition. If cleverly thought out, this approach enables both qualitative and quantitative evaluation of materials required to comprehend subtle trends in materials properties. Some successful combinatorial studies include design and development elastic polymers [17-20], active materials such as ordinary and ferromagnetic shape memory alloys [21-22], hydrogen storage materials [23-24] and novel fuel cell catalysts for energy research [25-26].

In combinatorial science, synthesis is often the easier of the two tasks to implement, although it certainly is not without challenges. As opposed to single material production, methods such as parallel synthesis allow generation of a large pool or libraries of candidate

materials in many industrial fields such as medical and pharmaceuticals. Alternately, the discrete combinatorial approach can be used to generate libraries of solid state materials with distinct compositions. By depositing multiple elements in sequential order to form a stack of elemental layers using a series of masks, a thin film array with hundreds of discrete compositions can be achieved. A comparable method involves deposition of varying metallic solid salt mixtures in sol-gel and patterning these compounds into arrays of small containers. The result is an ensemble of metal compositions prepared specifically for rapid characterization [1-2].

For thin film-based materials systems, the “continuous composition spread” technique is particularly useful. This approach offers a wide coverage in composition-space of the phase diagrams [13-16]. Physical vapor deposition techniques such as sputter deposition using direct-current (DC) or radio-frequency (RF) magnetron sputtering and pulsed-laser-deposition (PLD) offer a flux of atomic and/or molecular species from which films can be formed. A moving mask with a stationary sputter sources allows deposition of a film of varying thickness along the direction of the moving mask. If another element is sputtered on top of the first film using the mask traversing in the opposite direction, the result is a stack of film layers with two opposing wedges. Based on the speeds, directions and shape of the moving mask, and deposition rates of each sputter source, film compositions can be calculated as a function of position. Post-annealing then is required for inter-diffusion to ensure alloy formation between two different elements.

To circumvent the requirement for post-annealing processes, simultaneous deposition using multiple sources can be used to produce continuous composition spreads. Such codeposition offers many advantages over layered-wedged films obtained from sequential sputtering. Since codeposition yields films in an atomically-mixed, as-deposited state, annealing is not necessary, thus allowing the formation of low-temperature or metastable phases that cannot be achieved otherwise. The lack of shadow mask offers a simple and minimally cluttered design that also eliminates potential contamination problem from the mask itself.

Since physical vapor deposition techniques, such as magnetron sputtering, yield nonlinear deposition profiles, it is important to characterize the deposition profile for a given material as a

function of position on the substrate. Knowing the deposition profile enables fine control of film thickness and composition gradient across the substrate; our system is designed to achieve approximately 1 atomic %/mm composition gradient. Sliding-mask techniques have an advantage here since the composition gradient can be precisely determined and set by the velocity and geometry of the sliding mask, and the distances between the sputter source, the mask and the substrate.

1.5 HIGH-THROUGHPUT CHARACTERIZATION

Compared to synthesis, high-throughput characterization techniques are usually more challenging to develop. Since an overall process can only be as fast as the slowest step in the process, a slow evaluation method will defeat the purpose of creating an efficient characterization system. Therefore developing screening techniques and characterization methodologies requires careful design and planning. There are several considerations to keep in mind when choosing an evaluation method. With speed and efficiency being the keys to high-throughput evaluation, a number of methods can be employed to enable an effective overall characterization process. For example a parallel screening approach can be used for rapid identification of promising materials or trends, despite being more qualitative than quantitative. This might be followed by a serial interrogation of promising regions. Although slower, the serial technique might provide better resolution and more quantitative information. This intelligent combination of both approaches provides for rapid yet effective screening.

One scheme that is proving versatile at addressing difficult characterization problems is the development of MEMS-based investigation techniques. The use of an array of micromachined cantilevers as a substrate for sputtered composition spreads has been identified as a convenient method for probing physical properties. The technique is particularly well-adapted to the measurement of thin-film stress. For a composition-spread sample, different material compositions would coat the top surface of each cantilever, so each bilayer will respond independently to external stresses. Takeuchi et al. [13] have shown that this technique can be

used to map the transition temperatures of ferromagnetic shape-memory alloys for ternary composition spreads. To circumvent the short-fall of using large cantilevers with combined properties of compositions, we developed the high-throughput testing system suitable for thin-film mechanical and magnetostriction measurements of ternary composition spreads with 1 atomic % composition change per micromachined cantilever.

CHAPTER 2

GENERAL DESCRIPTION OF EXPERIMENTAL TECHNIQUES FOR HIGH- THROUGHPUT COMBINATORIAL STUDIES

2.1 INTRODUCTION

This chapter is the general description of the experimental techniques pertinent to the entire dissertation, and is divided into three sections. The first describes the methodology related to the preparation of samples and, in particular, explains and justifies the adopted techniques. This section also discusses the factors that influenced the choice of substrate platform and also describes the issues related to microfabrication of the sample platform. Additionally, this section discusses the spectrum of competing techniques and present an extensive review of film deposition techniques. Analyses using characterization tools such as nanoindentation, electron microprobe (EDX) and X-Ray diffraction (XRD) are also discussed. The second section describes the construction of the curvature measurement system. Because the construction of the system played a central role in the dissertation, each component pertinent to the design and building of the system is described and discussed in detail. Competing screening and characterization approaches are also reviewed, and the factors that have been evaluated during the decision-making process are discussed. The third section describes the theory of curvature measurement.

All sample preparation and measurements took place at Cornell University, with the exceptions of nanoindentation and some of the EDX and XRD measurements of Ni-Fe-Al ternary composition spread, which were conducted at the Eidgenössische Technische Hochschule (ETH) in Zürich. MEMS cantilevers were prepared in the Cornell Nano-Scale Science & Technology Facility (CNF) and thin films were deposited with our custom-built vacuum chambers in Bard and Duffield Hall. Film samples were characterized using EDX and XRD in the Cornell Center for Materials Research (CCMR) facilities. All high-throughput magnetic and mechanical measurements of thin films were carried out using our custom-built curvature measurement system. This system is capable of evaluating both composition spread and ordinary single-composition films. Specific experimental details performed during both residual stress measurements and magnetostriction measurements are described in Chapter 3 and 4, respectively.

2.2 SAMPLE PREPARATION FOR COMBINATORIAL SYNTHESIS

Sample preparation involved two major steps. First was the development of a substrate platform suitable for high-throughput thin film investigations. This portion of preparation, primarily the fabrication of substrates, required major efforts in innovation, materials analysis and methodologies to create a useful and reproducible substrate system. The intent was to design a substrate that was inexpensive and required a minimum effort to produce. While emphasizing economy and efficiency of fabrication, the other main factors influencing the choice of a platform were reproducibility of its sample size, composition makeup, structural integrity and surface uniformity. The films being measured must be deposited on a substrate that was chemically inert, structurally strong, and electrically insulating. Once fabricated, the substrate must be robust in order to be used in extreme conditions such as elevated temperatures and under large stresses. If fabrication process allowed flexibility in determining substrate feature size (e.g. cantilever dimensions, such as thickness, width and length), then thin films deposited on these cantilevers would have corresponding lateral dimensions. Ability to change cantilever dimensions would offer different sensitivity range or radius of curvature of measurement; thin and long cantilevers were compliant and sensitive, and thick and short cantilevers were to accommodate larger stress or higher magnetostriction.

The second part of sample preparation was the deposition of thin films onto the pre-fabricated substrates. In contrast to the first part, this portion did not require significant innovation as physical vapor deposition of thin films is well established. In this dissertation, single-compositions, binary and ternary composition spreads were studied. Analogous to spray painting, a single-composition thin film was obtained when the desired elemental material in a sputter-deposition source was atomized and allowed to condense onto a substrate, forming a thin layer. When multiple sputter sources were used (co-deposition), a thin film with varying composition was obtained. This composition gradient was achieved by taking advantage of deposition-rate variation due to directional effect of sputtering from the source onto a wide substrate.

2.2.1 Choosing the Substrate Platform

There were a number of candidates to be considered for the substrate platform. Traditionally a thin sheet of glass (such as a microscope slide) or a single-crystal silicon wafer would have been used as a host substrate for simple curvature measurements. The substrate must support the thin film and act as a counter-layer in a bimorph for probing the film stress. Therefore any number of thin metallic sheets with smooth surface might be a suitable choice. One potential candidate material was thin hot-rolled molybdenum (Mo) foil which could be used as substrate if advanced processing techniques such as photolithography-based microfabrication were not applicable. Thin Mo-foils with thickness of less than 10 mils (0.010 inch) were readily available from a number of vendors. If Mo-foils were to be used, these foils would be fully characterized to its product specifications, meaning its physical properties would be evaluated extensively, and costs associated with the entire process flow to fabricate each substrate would be carefully calculated. Alternative methods such as spark erosion and chemical etching could be used to fabricate desired substrate patterns or shapes directly from these raw Mo-foils. Despite these advantages, Mo-foils had many limitations. A particular concern was that the techniques for patterning these foils were not available locally. If device layout were changed to accommodate alternate characterization schemes, a new design for the substrate platform would need to be outsourced, potentially incurring excessive costs or time delays. The surface roughness and thickness uniformity of the foil may present a more fundamental limit to the usefulness of this material, depending on the deposited film thickness. The high conductance of Mo-foil may also interfere with electronic measurements.

The most prevalent equipment and sophisticated techniques available today in microfabrication are those related to silicon processing because of the widely used silicon processing in the IC and semiconducting industries. In particular, silicon micromachining is a high-precision fabrication technique that uses photo- or electron-beam lithography and various etching methods to form two- and three-dimensional structures in thin film materials. Micro- and nano-structures such as holes, posts, wells, pyramids, lines, grooves, hemispheres, and needles

are routinely patterned and fabricated with high reliability and precision. In the same way that Si has revolutionized the micro-electronics industry, this versatile material has also transformed into miniature mechanical components, devices and systems. Common examples of MEMS devices include microcantilever beams, tiny gears, valves, springs and tweezers, X-ray lenses, pressure and strain transducers, ink-jet nozzle arrays, electrochemical sensors, multi-socket electrical connectors, and force and acceleration transducers [1-2].

With the wide range of equipment readily accessible in the CNF, photolithography-based micro-fabrication techniques are the most versatile means to obtain a robust substrate platform. A wide range of wet and dry chemistries allows fabrication of substrate to be tailored as desired. The capacity to produce many distinct substrate configurations using various combinations of processes offers a rich and attractive alternative to the simpler planar configuration associated with Mo-foils.

Substrate reproducibility was a major concern from the measurement reliability standpoint. For example, even a minuscule variation in substrate thickness or surface roughness could result in parameter changes that could complicate subsequent analyses or produce misleading results. In addition, extra demand on the processing was that individual substrate of the platform must be small enough to contain minimal composition variation. This was extremely important for composition spread measurements because having multiple compositions on a single substrate (cantilever) would lead to a measurement of effects due to multiple compositions and would greatly defeat the advantage of composition spread measurements. For a high throughput automated measurement system, the substrates have to be either stitched together or multiple substrates must be on a single platform such as a Si wafer. With the availability of the state-of-the-art equipment in the CNF at Cornell University, the best approach is the development of a platform that contains an array of cantilever beams, each acting as an individual sample substrate for thin film analysis.

2.2.2 Designing the Cantilever Array Fabrication

Our overall approach to creation of a cantilever array is similar to that reported by Takeuchi, et al. [13], but is dramatically different with regard to the dimensions of the cantilevers, which introduces a number of unique issues that must be resolved. In both cases 75-mm diameter <100>-cut Si wafers are used as base substrates for the cantilever arrays. In Takeuchi's work, the structures are fabricated by bulk Si machining, resulting in cantilevers that are several millimeters in size and less than 100 per wafer. In contrast we have developed a unique fabrication process that produces arrays of cantilevers about tenfold smaller in size (e.g., 0.05 x 0.5 mm). The cantilevers are positioned on a square 1 mm x 1 mm grid to accommodate the predetermined compositional gradient of 1 atomic % change per mm for composition spreads. Over 3,000 cantilevers are produced on each wafer. The small size of the cantilevers enables the desired compositional uniformity of <1 atomic % across a cantilever. This is extremely important step towards achieving combinatorial studies of shape memory materials such as Ni-Ti based alloys, which have composition sensitivity on the order of half a percent. If an individual cantilever has a significant composition gradient on it, then data will be smeared out.

Importantly, the substrate platform must be inexpensive, since this platform was intended for high-throughput measurements. A wide variety of MEMS fabrication techniques were evaluated for the production of cantilevers, including alternative bulk micro-machined Si techniques, Silicon-on-Insulator (SOI) processed using HF etching, and deposited Si_3N_4 [ref]. Each approach requires a distinct process flow. Bulk micromachining of Si is useful in making thick cantilevers but often results in imprecise thickness (~10%), requires multiple lithographic steps and does not allow batch processing [27]. Although SOI does not require as many steps, it is relatively expensive (~\$200/wafer). We choose Si_3N_4 as cantilever material because it is straightforwardly processed in a batch process (~5 wafers/process cycle), so it is very economical (~\$35/wafer). The thickness of the nitride film can be controlled with high precision (<3%) when deposited by low pressure chemical vapor deposition (LPCVD), and the as-

deposited stress in LPCVD films can be tuned to a very small value by appropriate choice of process variables. The elastic properties of Si_3N_4 are well established and the Young's modulus is known to be 290 GPa [2].

A 1- μm -thick film of silicon nitride (Si_3N_4) is deposited onto the blank Si substrate by low pressure chemical vapor deposition. The cantilever pattern is written onto a quartz mask and transferred onto the Si_3N_4 using standard photolithography. Si_3N_4 is then etched by reactive-ion-etch (RIE) using fluorine chemistry. Once the underlying Si layer is exposed, a KOH anisotropic wet etch is used to release the cantilevers: this etchant preferentially attacks $\langle 100 \rangle$ planes over $\langle 111 \rangle$ planes [ref]. The Si $\langle 111 \rangle$ plane acts as KOH etch-stop which can be seen as slanted walls (dark regions in the optical micrograph) in figure 2.1. A CO_2 critical-point dryer (CPD) was used to dry and release the cantilevers to avoid sticking. Cantilevers are designed to have dimensions of $500 \mu\text{m} \times 50 \mu\text{m}$ and be spaced 1 mm apart in a square grid arrangement.

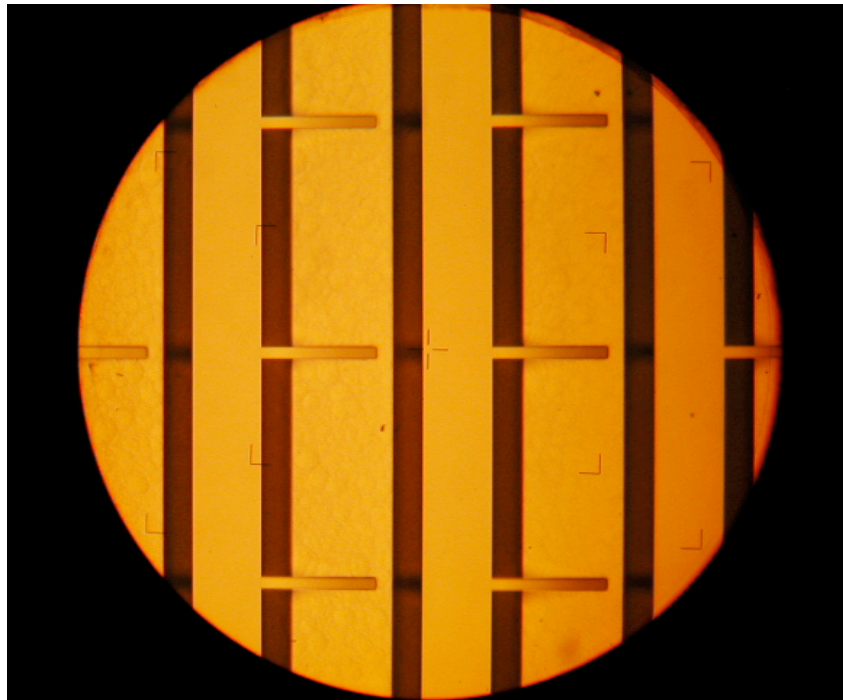
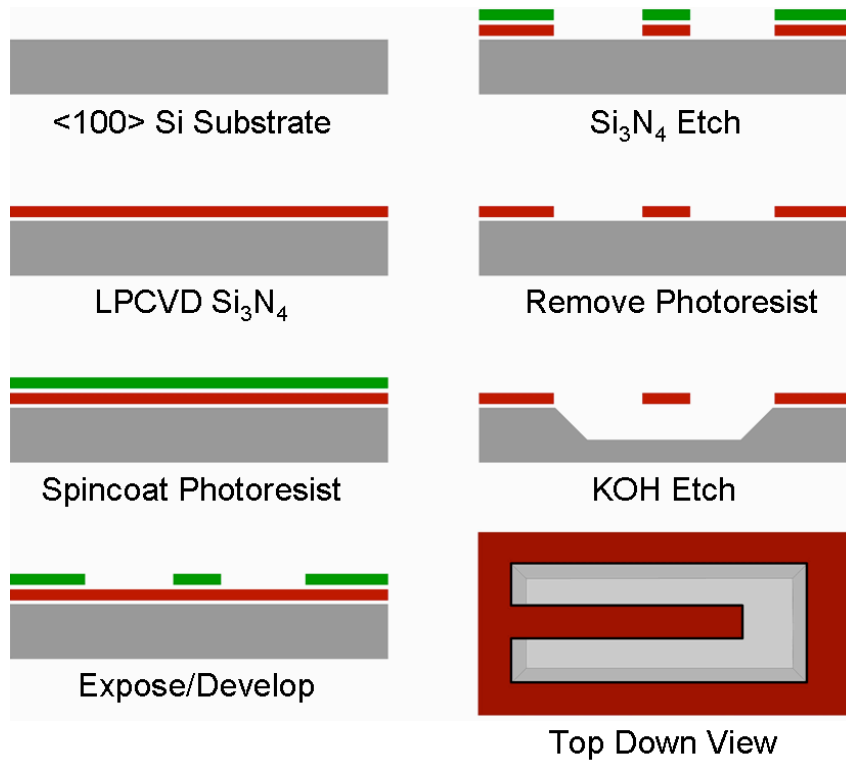


Figure 2.1: (Top) Fabrication process flow of a Si_3N_4 cantilever. (Bottom) An optical micrograph showing an array of released cantilevers. Vertical dark areas are slanted (111) planes of the Si base platform.

2.3 MICROFABRICATION PROCESS FLOW

2.3.1 Designing The Photolithographic Mask for Pattern Transfer

A number of computer programs are available for designing a custom mask for pattern transfer. L-Edit (Layout Editor by Tanner Research, Inc., CA) is a simple but powerful computer-aided design (CAD) program used to draw the layout for the cantilever array as well as for multiple-mask design required for 3D micro-structures. Figure 2.2 below shows a multi-mask CAD layout designed by the author for magnetic transducers for acoustic wave generation and detection.

Although numerous structural features, sizes and patterns were attempted for the mask pattern on the CAD program, only a few designs were written onto a physical mask. In designing a mask, it is important to consider all subsequent fabrication processes that will be carried out using it, as well as the limitations and effects of each process such as wet- and dry-chemistries and plasma etchings and depositions. For example, etching $\langle 100 \rangle$ silicon surface using KOH will give slanted silicon walls rather than vertically straight ones because KOH selectively etches $\langle 100 \rangle$ plane of Si; the slanted $\langle 111 \rangle$ plane acts as an etch stop. Thus, proper knowledge can help prevent wasting precious samples, time and money by troubleshooting improper designs.

2.3.2 Mask Generation of Cantilever Array Pattern

Once the CAD design is drawn, it is ready to be transferred onto a physical mask. Mask generators such as Heidelberg DWL 66 Direct Write Laser Pattern Generator and GCA 3600F Optical Pattern Generator are used in creating the masks. These tools use laser interferometry for accurate metering in the generation of patterns on Cr mask blanks. Used in standard photolithography, blank Cr masks typically have a photo-resist layer on top of 300-nm-thick Cr thin-film-coated quartz plate. The overall mask design can be written within a few hours on the blank mask. After the mask is exposed, it is developed with a mask developer solution and then rinsed with deionized water to form the pattern in photoresist. Cr etching is carried out using

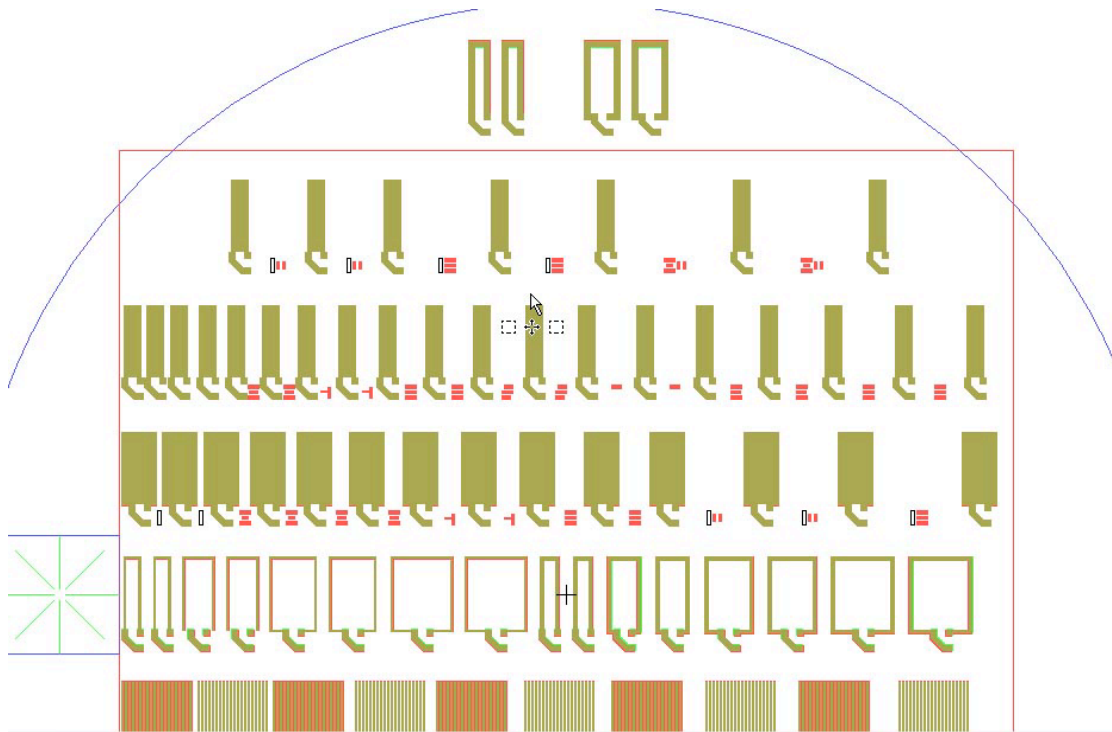


Figure 2.2: The layout of magnetically transduced surface acoustic wave devices. The layout contains two separate masks which are aligned using the alignment mark on the leftside of the layout pattern.

photoresist as mask and followed by resist-stripping as a final step. The finished product is a photolithographic mask (photo-mask) made of quartz with a geometric design patterned in Cr.

2.3.3 Photolithography – The Pattern Transfer from Mask to Substrate Platform

Photolithography, as the name suggests, indicates writing or patterning using light as a transfer medium. By blocking portions of light, a geometric pattern from a photo-mask is transferred as dark and illuminated areas onto the substrate. When photoresist is used, the light-sensitive organic chemical in the resist reacts with the intense ultraviolet (UV) light to form insoluble cross-linked regions of conjugated polymers in an otherwise soluble film. Essential components in photolithographic tools include a UV-light source, a mask holder and a substrate holder.

Two types of lithographic tools are widely available in fabrication laboratories. Contact-aligners are based on contact printing approach which is used when the mask and substrates are in close-contact. This mode enables patterns to be directly “copied” when exposed to the UV-light. The resolution of contact-aligner is limited by the wavelength of the light (~0.3 micrometer), but in reality is determined by the thickness of the photo-resist (~1-2 micrometer). The other tool widely used is based on projection lithography. This approach does not require the mask and substrate to be in close proximity, but rather at a distance that allows the set of optics to be used to magnify or reduce the mask pattern as needed. One advantageous feature of projection lithography is the ability to transfer smaller and finer feature sizes by magnification or reduction. Repeated stepping and projecting of the reduced mask-pattern onto the substrate allows producing of multiple devices/patterns per substrate. These so-called “steppers” are ubiquitous in microelectronics industry due to their ability to manufacture multiple devices on a single substrate wafer.

Photolithography tools are usually used in the first step of a long series of fabrication process. When using steppers such as 5x or 10x projectors, device dimensions are carefully calculated to foresee pattern shrinkage. Otherwise if an error is made on the photo-mask, the defect feature may be propagated through the entire fabrication process to give dysfunctional devices. Despite the high risk, photolithography offers uncompromised reproducibility of

substrate platform. Each substrate produced can be assured to have identical features as the next one.

2.3.4 Low Pressure Chemical Vapor Deposition of Silicon Nitride (Si_3N_4)

The LPCVD process enables deposition of ceramic and semiconducting materials at high temperature to achieve low stress films such as silicon dioxide and silicon nitride. Although not as commonly used as silicon dioxide in microelectronics, silicon nitride offers a particularly important set of properties that the oxide cannot match. Due to its stronger resistance to etchants such as potassium hydroxide (KOH), superior thermal stability, better diffusion barrier, higher hardness and strength, Si_3N_4 was chosen as the cantilever beam material.

Surface cleanliness is a major factor in obtaining optimum silicon nitride films. If the initial surface is not atomically clean, the role of surface defects may dominate the film characteristics. Therefore, prior to depositing silicon nitride, bare silicon wafers are dipped into a base pool containing 1:1:5 solution of $\text{NH}_4\text{OH} + \text{H}_2\text{O}_2 + \text{H}_2\text{O}$ at 75 or 80 °C to strip away all the contaminants on the surface. The cleaned wafers are subsequently transferred into an acid pool containing hydrofluoric (HF) acid to etch away the native oxide (usually a few nanometers) present on the surface. After rinsing, the bare silicon wafers are then placed in the loading-boat for nitride deposition.

A unique LPCVD deposition recipe was selected for deposition of silicon nitride. Since the deposition process carried out using the high-temperature nitride furnace in the CNF permits batch processing, depositing Si_3N_4 on 25 wafers per process cycle significantly lowers the cost of silicon nitride films. Depending on the type of silicon nitride desired, a number of different reacting gases such as dichlorosilane (SiH_2Cl_2) and ammonia (NH_3) can be used. The gases used in this process are solely handled by the CNF staff (for safety of operation) and as a result, composition uncertainty was minimized. Low stress silicon nitride recipe operated at 800 °C with a gas ratio of approximately 6:1 between SiH_2Cl_2 and NH_3 is used to obtain 200 MPa of tensile stress and index of refraction 2.2.

2.3.5 Reactive Ion Etching

Reactive ion etching (RIE) uses a reactive plasma combining chlorine (Cl) and fluorine (F) species to selectively remove material. Gas-phase carbon tetrafluoride (CF₄) is used to anisotropically etch silicon nitride. Photoresist is commonly used as etch-barrier in RIE, although this material is also etched, albeit at a slower rate. Typical etch rates for silicon nitride are approximately 22 nanometers per minute. An etch selectivity of 1:1.67 to photoresist is typically obtained.

2.3.6 Wet Etching – KOH

Wet etching refers to an aqueous chemical reaction that removes a particular material. Potassium hydroxide (KOH) is a strong base widely used in etching of silicon wafers. The hydroxide ion (OH⁻) in the KOH solution attacks the <100> plane of silicon crystal much more rapidly than the <111> plane. The selectivity between the two planes is on the order of 400:1 favoring <100> plane. As seen in the figure, 50% KOH solution in deionized water offers a wide range of etch-rates for the <100> silicon surface.

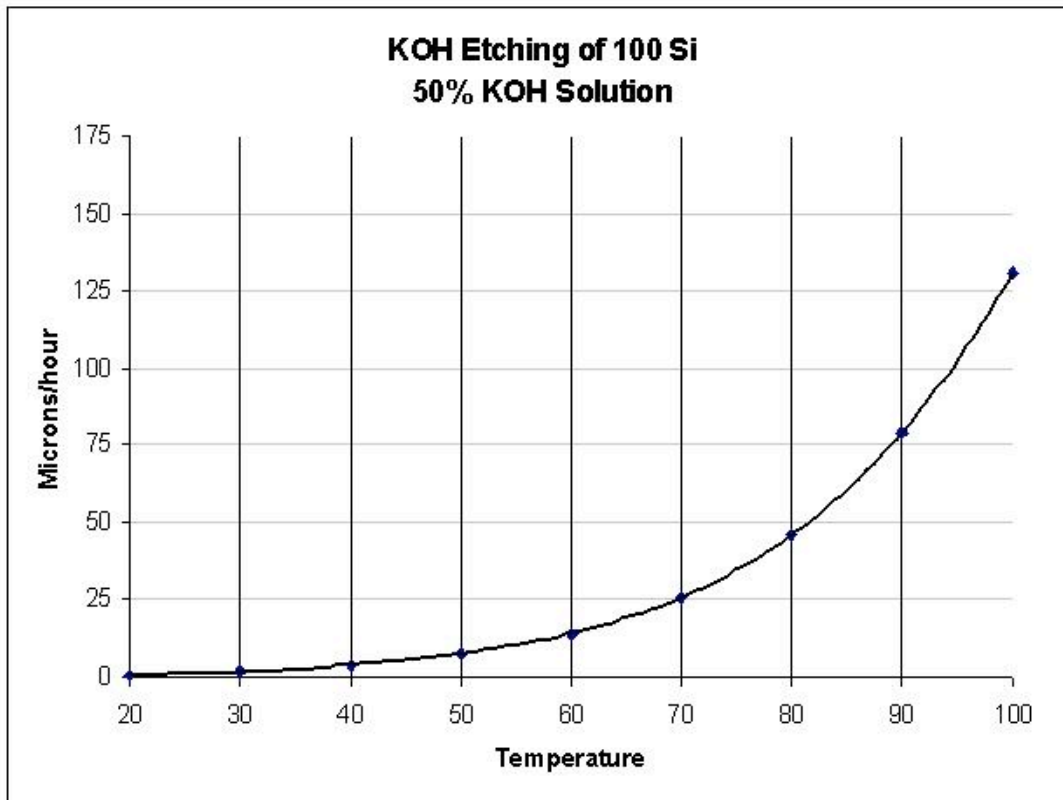


Figure 2.3: KOH etching rate versus temperature for 50-50 solution of KOH and H₂O.

This plot in figure 2.3 does not show the roughness of the etched surface of the Si planes. This trade-off between etch-rate and surface roughness must be considered when choosing the process condition. Depending on the etch parameters, an extremely smooth surface can be obtained at the extremely slow pace or faster etching can be obtained at the cost of smoothness. As for the substrate platform, a reasonable etch rate of 75 micrometers per hour at 90°C gave relatively smooth surface-finish that was sufficient for our purposes.

The procedure involved in KOH etching includes continuous stirring and temperature monitoring. Constant removal of etched materials in the solution permits steady etch rate. The amount of solution should be maintained to a constant level by adding deionized H₂O as needed. Replenishing is necessary to maintain the chemical ratio and to help regulate temperature. Temperature monitoring includes measuring the temperature with a thermometer and controlling

the heat source (hot-plate) through a feedback system. A closely controlled temperature is necessary to achieve accurate etch-rate and desired surface roughness. Once etching is finished, substrates are rinsed several times with deionized H₂O at 4 successions of temperature of 90°C, 60°C and 40°C and 23°C. If rinsed immediately after the etch with room temperature H₂O, the sudden change in temperature can cause thermal shock and structural damage.

2.3.7 Critical Point Drying

After KOH etching, the released cantilevers must be dried using a critical point drying (CPD) process. If substrates are left in air for slow evaporation, the surface tension of the water film will pull the released cantilevers down to the bottom of the pit. The result is a substrate full of cantilevers stuck to the bottoms of the etch-pits. These cantilevers are too small to pry out using a set of tweezers, and even if it is possible to do so, manually releasing over 3,000 cantilevers would take months to accomplish. Attempting to blow-dry the cantilevers will only result in broken cantilevers.

Before CPD, substrates are rinsed thoroughly in 4 steps to remove residual water and contaminants. The first step is rinsing with a mixture of 50% deionized water (H₂O) and 50% methanol (MeOH). The second rinse is with 25% H₂O and 75% MeOH. The third step is a 100% MeOH rinse. As the final step, substrates are submerged in 100% MeOH before transferring to the CPD chamber.

Immediately after stacking substrates using Teflon rings as separators inside the CPD chamber, MeOH is poured inside the chamber to immerse the substrates to prevent them from exposure to air. The CPD chamber lid is then tightened to prevent explosion during high-pressure critical point drying process. During the purge cycle of the CPD process, liquid CO₂ replaces MeOH as the solution. The chamber is then pressurized to over 74 atmospheres and heated above 31°C to bypass the critical point of CO₂. After slow de-pressurization and cool-down, clean, dry, unstuck substrates are ready for the next step in the process.

2.4 SPUTTER DEPOSITION OF COMPOSITION SPREADS

Composition spreads are prepared using well-established thin film deposition techniques [15-16,28] to synthesize a wide range of compositions in a single experiment. To achieve ternary composition spreads, the deposition system is setup using three DC magnetron sputtering sources (sputter guns) (US Gun II, US inc, San Jose, CA) mounted at the vertices of an equilateral triangle (Fig 2.4) with the targets parallel to the substrate (nominally on-axis sputtering). The sources have been found to not interact with each other, so we can infer the position dependence of composition of the co-sputtered film by referring to the position-dependent deposition rates measured for each element individually. The power supplied to each sputter-gun can be varied to obtain the desired deposition rate from each gun. Thus the composition at the center is easily determined once the deposition rate of individual sputter source is measured. For example a film with 1:1:1 Fe:Ni:Al composition ratio can be produced straightforwardly by tuning each source to the sputter power necessary for equal deposition rate among the sources. Depending on the type of material being sputtered, the composition gradient changes slowly as the film tapers off towards the edge from the center of the substrate (Fig 2.4). If a higher gradient is desired, the substrate can be placed closer to the sources. The composition gradient we obtain is approximately 1 atomic % per millimeter, and thus allows deposition of distinct compositions onto each cantilever at increments of roughly 1 atomic %.

Fe-Ni-Al ternary composition spreads were deposited on prefabricated MEMS cantilever arrays to explore magnetostriction and to demonstrate the ability to map residual stress in ternary composition-space. Single composition films of $\text{Ni}_{60}\text{Fe}_{40}$ were deposited using an S-gun (Sputtered Films, Inc., Santa Barbara, CA) for use in calibration of the high-throughput measurement system for saturation magnetostriction and magnetostrictive susceptibility measurements. Binary composition spreads of Ni-Fe were prepared to demonstrate the ability to analyze simple trends. Films were prepared at various argon pressures and temperatures in order to determine conditions that yielded minimal observable intrinsic stress, or samples that have cantilevers with the least deflection.

2.4.1 Sputter Deposition System

All film deposition takes place using physical vapor deposition inside custom-built vacuum chamber. It is located in Bard Hall room 163 and used by multiple graduate students. Its cylindrical stainless steel body is approximately 27 inches in diameter and 15 inches tall. The sputtering guns are mounted on either 8-inch or 10-inch flanges on the side of the chamber and the chamber has a top lid operated by a mechanical hoist. The lid is lifted for access to the sputtering guns and substrates and for cleaning purposes, and is otherwise sealed so that the chamber is always under low vacuum pressure (pumped down) around 1 μ Torr.

The sputter chamber has several flanges on its side-wall available for housing various apparatus. A 10-inch flange mounted on the chamber is the home to the three sputter-guns located 2.5 inches away from the center of the flange (Fig 2.4 top). Each sputter-gun holds a 2-inch diameter target of the material of interest and cooled by closed-loop running water at 17-18 °C. The sputter guns are powered by DC power supplies that can be operated at constant power, constant current or constant voltage mode. This three-gun assembly is used in deposition of binary composition spreads containing Ni and Fe, and ternary composition spreads of Fe, Ni and Al. However, this setup is not so useful if uniform single composition film is desired because the substrate is off-center when a single sputter gun is used.

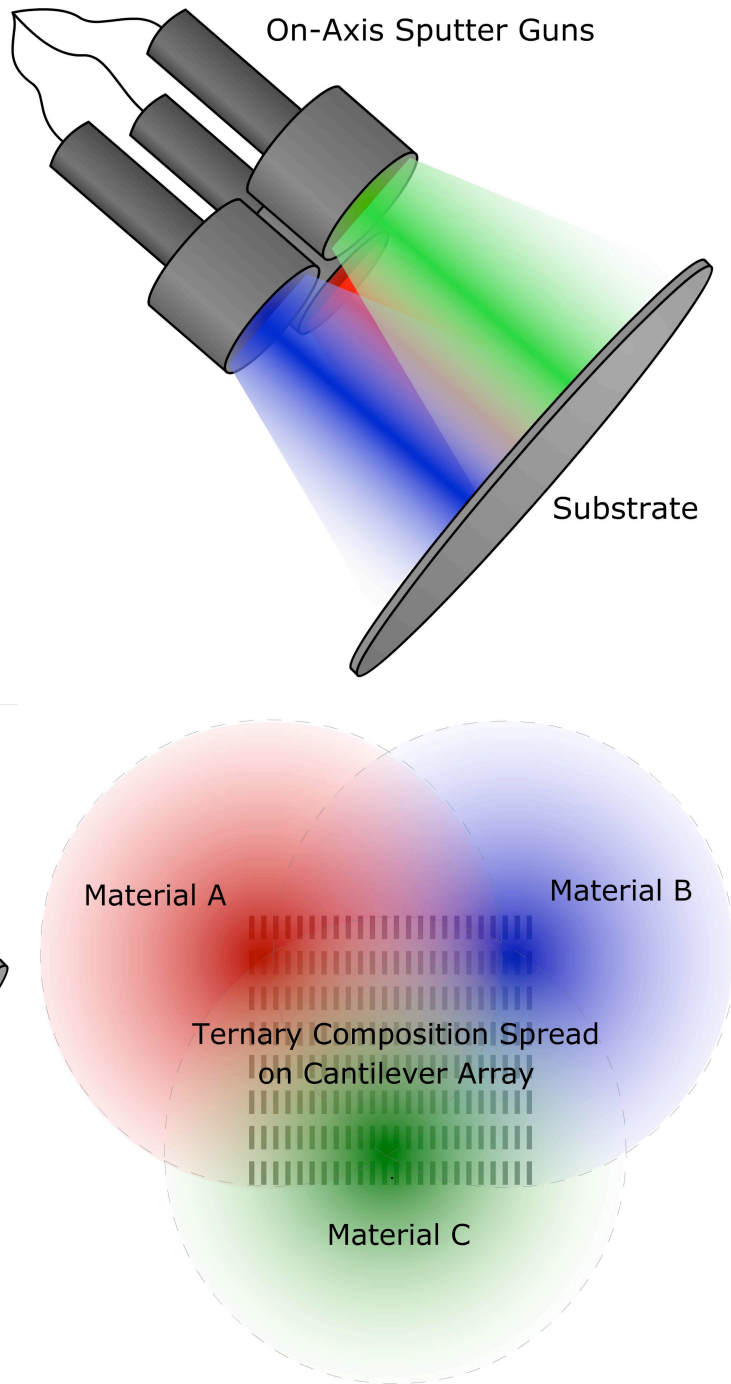


Figure 2.4: (Top) The three-gun sputtering setup used in co-deposition of the ternary composition spreads. (Bottom) A schematic representation of a ternary composition spread over an array of cantilevers; the variations in color intensity illustrate that thicknesses of the film also vary as a function of position.

For single composition films, a fourth sputter gun is used. The standalone S-gun (Sputtered Films, Inc., Santa Barbara, CA), specifically designed for sputtering of magnetic materials, is mounted on the opposite side of the chamber from the three-gun cluster described above. The S-gun is mainly used in producing magnetic thin films; however it is also occasionally used to produce underlayers of uniform thickness and composition because it is aligned to the center of the substrate when the substrate is moved directly in front of it.

The substrate holder is suspended from the center of the vacuum chamber lid with housing for electrical cables and water lines. The rotatable holder is designed for 3-inch substrates and smaller samples that can be mounted on the 3-inch substrate chuck. When facing the three-gun assembly, the substrate is approximately 1.5 inches from the targets to achieve a desirable composition gradient (Fig 2.4 bottom). When facing the S-gun, the substrate is approximately 5 inches from the target to achieve uniformity in thickness. The holder has a heater that allows deposition at temperatures up to 600 °C. A Variac autotransformer is used to supply AC power to the resistive heater attached to the substrate holder. The temperature is monitored using type-K thermocouple and is regulated manually with the Variac.

During pump-down, the chamber is rough pumped with liquid nitrogen (LN₂)-cooled sorption pumps from atmospheric pressure to approximately 100 milliTorr. The pressure is monitored using a Baratron capacitance manometer (MKS Instruments, Wilmington, MA). Below the crossover point of 1 Torr, liquid helium (LHe)-cooled Helix-cryogenic pump (formerly of CTI, now Brooks Automation, Inc., Chelmsford, MA) evacuates the system, typically down to a base pressure of a few μTorr. A Bayard-Alpert ionization gauge (Stanford Research Systems Inc., Sunnyvale, CA) is then used to monitor the base pressure subsequently to pressure as low as 10⁻⁸ Torrs, except during the deposition.

When desired base pressure of roughly 2 μTorr is reached after a few hours of pumping, the chamber is ready for sputter deposition. The low base pressure means the concentration of oxygen and water molecules inside the chamber is low enough that films will not be readily oxidized. To ensure oxidation is minimized, a sacrificial deposition of titanium is carried out for

several minutes to remove remaining oxygen from the chamber; titanium oxidizes readily during sputtering. Prior to the start of depositions, the flow rate of Ar is regulated by a mass-flow controller. Argon is required to sustain the plasma during deposition, and the Ar pressure can influence the film microstructure. During deposition, the Baratron continuously monitors the chamber pressure (mainly Ar gas) and the Ar flow rate is continuously adjusted to maintain a preset pressure. The operating gas pressure of 10.0 milliTorr is used as a standard condition in most depositions and especially in deposition of uniform single composition films. However the Ar pressure can be varied in attempts to achieve low stress films and desired microstructures.

2.4.2 Sputter Deposition Profile

Prior to film deposition, the deposition rate of each target is characterized as a function of power or current supplied while keeping other parameters constant. These data are then used as a guide to determine composition ratio when composition spreads are prepared. There is no significant difference in deposition characteristics between constant applied power and current, but to follow precedence, constant current operation was chosen.

The first step in characterization uses a crystal rate-monitor located at the exact location where the substrate will be. The crystal monitor is a 10-millimeter diameter quartz crystal oscillator which measures the shift in resonant frequency due to mass change. The frequency shift is directly related to the accumulated mass, so that the total thickness and deposition rate can be calculated using the density and molecular mass of the material [29]. The measured deposition rate versus applied current is then used to serve as a guide in subsequent depositions.

After all materials are characterized, the power supplies are programmed to supply the exact currents needed to achieve the desired composition ratio. Films are typically designed to have a 1:1:1 composition ratio; however any ratio is possible. To obtain a certain film thickness, the material with the lowest deposition rate at a reasonable applied current is used to calculate the deposition time. If the sputtering time is too long (i.e., on the order of hours), then the next

higher set of currents is used. The lowest rate is chosen because operating at maximum current is dangerous and shortens the life of the power supplies.

The crystal rate-monitor generates relatively accurate deposition rates at the center of the substrate, but does not measure rates at off-center positions. If the rate monitor were small enough (~1 millimeter) and able to be repeatedly re-positioned to determine deposition rate of every square millimeter space diagonally along the substrate, then spatial dependence of deposition rate can be “mapped.” This process could be done efficiently if the crystal rate-monitor was mounted on a positioning stage but the system is not equipped with such a stage. An alternate method is employed to achieve the same goal. This method involves deposition of the trial film on a substrate coated with a thin (~3 millimeter width) wax line diagonally across its surface. When the wax is removed with trichloroethylene, the deposited film on top of it is “lifted off,” leaving behind a film bisected by a groove of exposed substrate. The film thickness is then quantified with a physical stylus profilometer. The measurements are taken across the groove at 1-millimeter increments to give the thickness a function of position. The radial symmetry of the deposition profile allows the thickness profile to be applied to the entire substrate.

2.5 THIN FILM CHARACTERIZATION

Film characterization is carried out once a region on the composition spread with interesting properties is identified. Various established experimental techniques are employed to characterize the film crystal structure, composition, and surface properties. Energy Dispersive Spectroscopy (EDX) is used to confirm elemental compositions at selected positions with ~1 micrometer resolution. X-Ray diffraction (XRD) is used to obtain phase and structural information for the composition spreads [30-31]. The incident x-ray beam is approximately 1 millimeter x 3 millimeters, so this measurement averages over a region of the sample with a small range of compositions. Nanoindentation techniques are employed in determining

mechanical properties of materials such as modulus and hardness. Scanning electron microscopy and optical microscopy are used to image samples with high resolution.

2.5.1 Electron Microprobe - EDX

Electron microprobe equipped with energy dispersive spectroscopy is used to determine the compositions of combinatorially prepared film. A high energy focused electron beam is used to generate X-rays characteristic to the elements present in the sample. These characteristic X-rays, through quantification of elemental ratio in the composition, are used for chemical analysis. The focused electron beam is usually rastered over a small sample area to determine average composition; its composition measurement error is on the order of 5-10 % and typically higher when neighboring elements in the periodic table are present.

2.5.2 X-ray Diffraction - XRD

X-Ray Diffraction is used in studying crystallographic properties of composition spreads. In order to extract phase and structural information, the films have to be crystalline. Amorphous samples are not periodic and d -spacing cannot be determined from diffraction. Annealing amorphous films at high temperatures can crystallize the samples in order to be used in XRD experiments. Measurements of a crystalline sample are taken as diffraction peaks versus angle between the X-ray source, the sample and the detector. The collected “X-ray peaks” are compared and matched with the known peaks in the database to quantify the phase and structural properties of the material. The incident x-ray beam is approximately 1 millimeter x 3 millimeters, so this measurement averages over a region of the sample with a range of compositions.

2.5.3 Nanoindentation

Mechanical properties such as Young’s modulus and material’s hardness can be determined by nanoindentation. This technique is especially useful when investigating material

properties in extremely small dimensions – perfect for composition spreads with composition gradient of 1 atomic % / millimeter or smaller. In order to determine residual stress of a film composition using Stoney’s formula [32], Young’s modulus needs to be determined beforehand. A hard tip, typically a diamond, is pressed into the film with a known load. Displacement as a function of load is measured. From each displacement value, the area of indent can be inferred if a geometrically characterized tip is used (Fig 2.5). Then the resulting relationship between load and displacement (surface area) is used to obtain Young’s modulus.

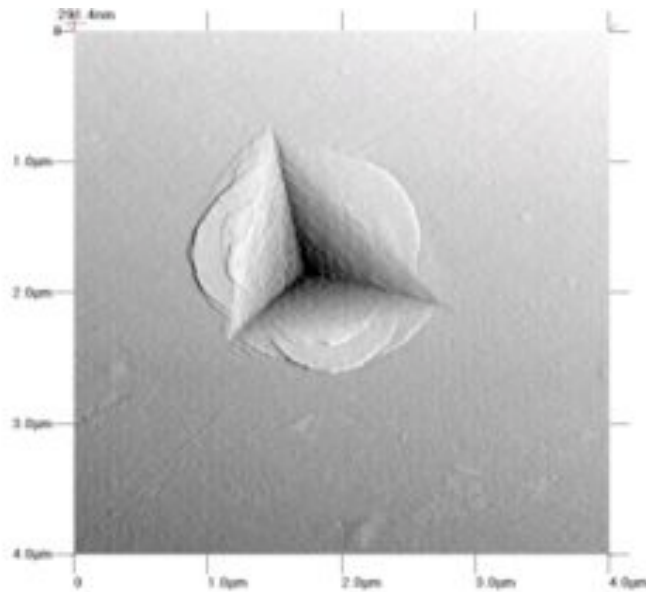


Figure 2.5: An AFM image of an indent left by a Berkovich tip.

2.5.4 Scanning Electron & Optical Microscopy

Images of samples are taken using scanning electron and optical microscopy. Images provide immediate information of the stress of the films being deposited. For example, the SEM image (Fig 2.6 top) can be used to determine the radius of curvature of the deflected cantilever: In this case the radius is 19 μm , not taking into account distortion due to the slightly tilted

perspective. The intrinsic stress from film deposition causes the cantilever to bend upwards; positive curvature means the film is under tensile stress. The large curvature of this cantilever shows that the stresses are too large and cantilevers are deflected too high to be able to use in the high throughput measurement system. On the other hand, the optical image in figure 2.6 bottom shows an array of cantilevers under low compressive stress. The slightly darker tips of the cantilevers mean they are reflecting light away from the microscope objective; the small difference in gray-level implies that cantilevers are slightly deflecting downwards. Therefore this image establishes that the curvatures of the cantilevers are small enough to be used in the high-throughput measurement system.

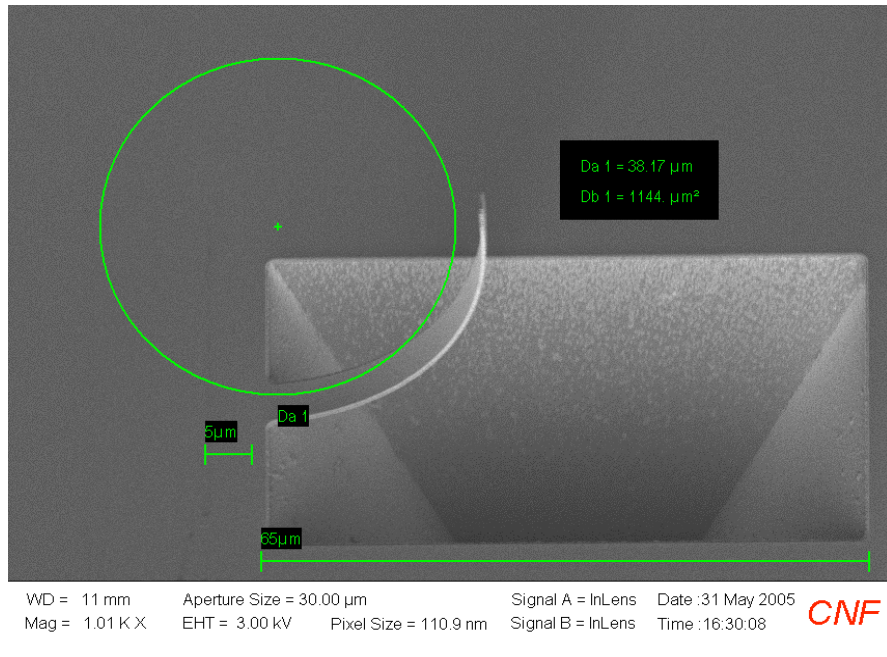


Figure 2.6: (Top) An SEM image of a bent cantilever exhibiting that large radius of curvature due to high intrinsic tensile stress. (Bottom) An optical image of an array of compressive cantilevers at 1 mm x 1 mm grid. Vertical dark lines are slanted $\langle 111 \rangle$ etched planes of Si.

2.6 INSTRUMENTATION FOR CURVATURE MEASUREMENT

The main idea behind measuring curvature of a bending bilayer structure is to determine stress-induced differential expansion between the two layers either from intrinsic or by an external force [32-37]. Using silicon nitride as the base layer cantilever beam, stress measurement experiment is developed to investigate mechanical properties of thin film materials through static bilayer deflection. Using the well-established Stoney formula [38] to relate curvature to mechanical properties of the materials, one can systematically determine film's modulus, stress, and other physical properties relatively straightforwardly. After measuring each cantilever in the composition spread, a ternary phase diagram of residual stress as a function of composition can be obtained. For magnetostriction measurements non-magnetic base layer of silicon nitride is also required to isolate the property of interest. During the measurement, imposing magnetic fields from orthogonal Helmholtz coils cause each cantilever to bend distinctly due to composition difference. Curvature changes due to magnetostriction are then optically detected and the resulted correlated cantilever tip deflections yield corresponding magnetostrictive coefficients through a derived relationship between curvature and the magnetostriction coefficients.

Overall measurement setup is similar for the two sets of experiments; extra components in magnetostriction are the inclusion of a set of orthogonal Helmholtz coils. Both have two major components: 1) the position sensitive detection (PSD)/data acquisition system used to measure the angular deflection of the cantilever at a selected spot, 2) the precision linear translation stage used to map the wafer, as illustrated in figure 2.7. LabVIEW[®] [National Instruments Corporation] computer program is extensively used to control the various components of the measurement system and integrate them with a Virtual Control Interface (VCI). The workflow consists of an initial calibration/registration, followed by fully automated data acquisition and cantilever maneuvering.

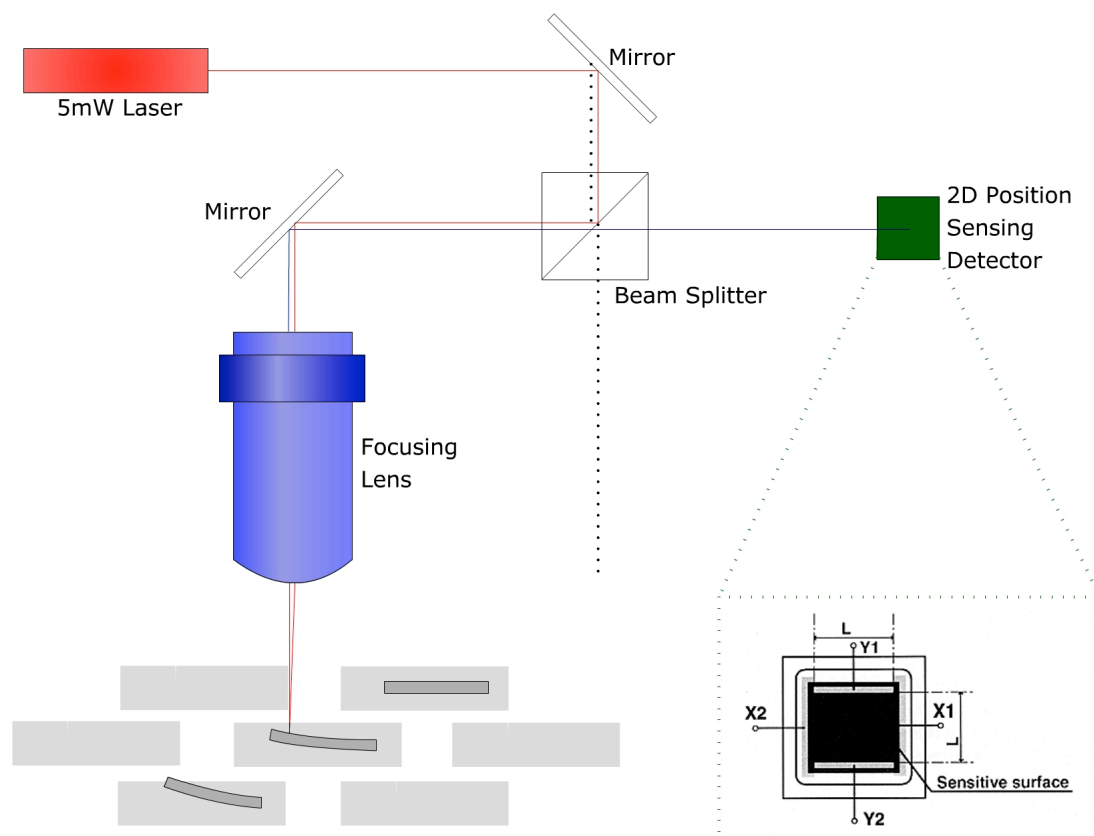


Figure 2.7: Cantilever curvature measurement setup. Laser light is directed through a series of lenses and mirrors, and microscope objective lens is used to focus the beam small enough to scan along the cantilevers. Reflected light is read by PSD and processed by VCI.

The optical detection system consists of a laser that is focused down to a laser spot (<50 micrometer diameter) using a 25x microscope objective lens (Fig 2.7). The setup also includes a pin-hole aperture, mirrors, 50%-50% beam splitter, and a 2D position sensitive detector (PSD) with linearity better than 99.95% over 80% of the active area [39]. The PSD measures the deflection of the reflected laser beam and is interfaced to the computer using an A/D converter.

Two precision linear translational stages [MICOS GmbH, Germany] with 1 μm accuracy are controlled using a serial bus interface RS232 integrated into the VCI. The stage is programmed to do a variety of tasks including scanning along a specific direction and/or in a grid. The resolution of the stage enables precise alignment with respect to the tip of the cantilever. Accurate alignment across the entire cantilever array is crucial. Therefore, prior to scanning, a registration/calibration procedure is executed to determine the exact position of two reference points located diametrically across the array grid. Once the reference points are located, every other position on the array grid can be interpolated since the exact positions of all the cantilevers are defined by lithography. Measurements for each cantilever are collected into a file, which is then analyzed using a MATLAB[®] [The MathWorks, Incorporated] script to calculate the desired property in either residual stress or magnetostriction coefficients. From these data sets, contour plots and phase diagrams are generated.

2.6.1 LabView Integration - Virtual Control Interface

To systematically investigate the properties of thin film composition spreads, a number of various components are integrated in the LabView graphical programming software. All the control and movement of the micro-stages, energization of the Helmholtz magnetic coils, and control of A/D equipment are entirely incorporated in LabView graphical programming interface and designated as Virtual Control Interface. Data analysis is carried out using coded scripts in MatLab program whose purpose is to generate phase diagrams and contour plots using data acquired from the VCI. The idea is to automate as many functions as possible so as to necessitate minimal manual input. The entire measurement operation can be conducted by first mounting a sample wafer fully covered with a thin film composition spread coated on microfabricated cantilevers onto the micro-stage, and then pressing a single button to acquire all the necessary data to generate ternary diagrams. The program is designed to be effortless and to work as smoothly as possible between data acquisition and analysis. Perhaps the most unexpected positive outcome of working with composition spreads is exclusion of unwanted run-to-run variation in experimental conditions which is generally found to be a major source of uncertainty and error. With automated generation of these ternary diagrams of the properties being probed, the high-throughput analyses of thin film composition spreads has become a resounding reality.

As mentioned in the overview of instrumentation setup, the VCI is divided into two major components: one is the x-y stage control and the other is data acquisition from the position sensitive detector (PSD). These two parts are fully integrated in the LabView program. An additional controller for a set of Helmholtz Coils for magnetic measurements is also integrated into the VCI, although this subsystem has not been automated. Other major components of the measurement setup that are not part of the VCI include the modulated diode-laser system, mirrors, focusing and condensing lenses, beam-splitter, pin-holes, and vibration-isolating air-support stage to filter out low frequency noise.

2.6.2 Optical Measurement Setup

The optical measurement setup consists of a moderately coherent elliptical beam obtained from 5-mW diode laser (StockerYale Inc., USA) or a circular beam from a 4-mW He-Ne laser (Metrologic Instruments, USA), a set of mirrors, lenses and an objective lens to guide the laser beam onto the sample. The reflected laser beam is directed through a 50% beam splitter to the photosensitive detector using mirrors. The key component of the optical measurement scheme is the 2D-Duolateral photosensitive detector (On-Trak Photonics, USA).

2.6.2.1 Position Sensitive Detector - PSD

The PSD is a photo-sensitive silicon chip with a 4 millimeters x 4 millimeters responsive area. This chip has sufficient sensitivity to trace the position of the deflected laser beam. By placing it directly behind the beam splitter in line with the objective lens, the relative change in PSD voltage due to the change in direction of the deflected beam from the initial one can be used to determine the angular deflection, and hence curvature change of the cantilever in magnetostriction measurements. Measuring the relative change in the deflected laser beam between the base of the cantilever and the tip allows us to infer the static curvature of the cantilever which is used in determination of residual of stress measurements. If higher sensitivity is required or deflection is too large to be detected in the PSD – meaning the beam has spilled off the detector— adjusting the distance between the PSD and the sample can offer a trade-off between high sensitivity and bigger range of measurement. For large (out-of-range) deflections a simple expedient is to measure closer to the base of the cantilever where a smaller incline angle obtains.

Calibration of the PSD is carried out by determining the direct relationship between the PSD voltage change due to a change in the inclination angle of the sample. This voltage-to-angle relationship eliminates the need to determine curvature change of the cantilever beam for small angles. Typically, a reflective sample such as a SiO₂-coated wafer or a mirror is carefully angled such that the reflecting plane is at the same position as that of a real sample. The distance

between the objective lens and the sample is compensated to correct for any significant changes in the focal plane. The angle of the reflected wafer or mirror is systematically varied and the corresponding PSD voltage measured. This calibration step is required for quantitative measurements after every modification of the optics system. The calibration of the finalized optical system must be verified only occasionally.

2.6.2.2 Objective Focusing Lens

A 25x microscope objective lens is used in focusing the incoming laser beam. Since the dimensions of cantilevers are on the order of tens of micrometers, the laser beam size must be equal to or smaller than the cantilever dimensions $< 50 \mu\text{m}$. Spilled or strayed light reflecting off of cantilever adds error in the measurements and must be carefully avoided. An adjustable pin-hole aperture is placed in and out of the beam-splitter to eliminate all strayed light coming from sources other than the laser beam.

2.6.2.3 Beam Splitter

Directly in front of the objective lens is a 50%-50% cubic beam splitter (ThorLabs Inc., USA). Measuring small angle deflection of the cantilever requires the incident and deflected beam to be almost on the identical light path. The sheer physical size of the objective lens prevents employing individual lenses for magnification and for collection of the laser beam. As a result using a single objective lens for both purposes is feasible. However in order to employ a single objective lens, a beam splitter must be used to allow superposition of the light path between the incident laser beam and the exiting deflected one. This is otherwise unattainable because the laser and PSD cannot be on the same path—they would block each other.

2.6.3 Helmholtz Coils Control – (for Magnetostriction Measurement)

Figure 2.8 shows the entire optical measurement set up inside two orthogonal sets of Helmholtz coils used to provide uniform magnetic field required for magnetostriction measurements of the composition spreads. One set of Helmholtz coils has smaller diameter than the other, enabling the smaller set to remain housed inside of the other. The coils are supported by Teflon frame and assembled on vibration isolation air-table to minimize low frequency noise. The Helmholtz coils are powered by two DC power supplies which can provide up to a maximum of 25 Amperes and 50 Amperes. A digital to analog (D/A) converter is used to control the power supplies using the VCI - LabView program. Although two DC power supplies are available, in some experiments, only one power supply is used for both sets of the coils. Manual switching between the two coil sets is done using a knife-switch or solid-state relay. In other experiments, each power supply powers a set of coils simultaneously to sweep the magnetic field azimuthally in the sample plane.

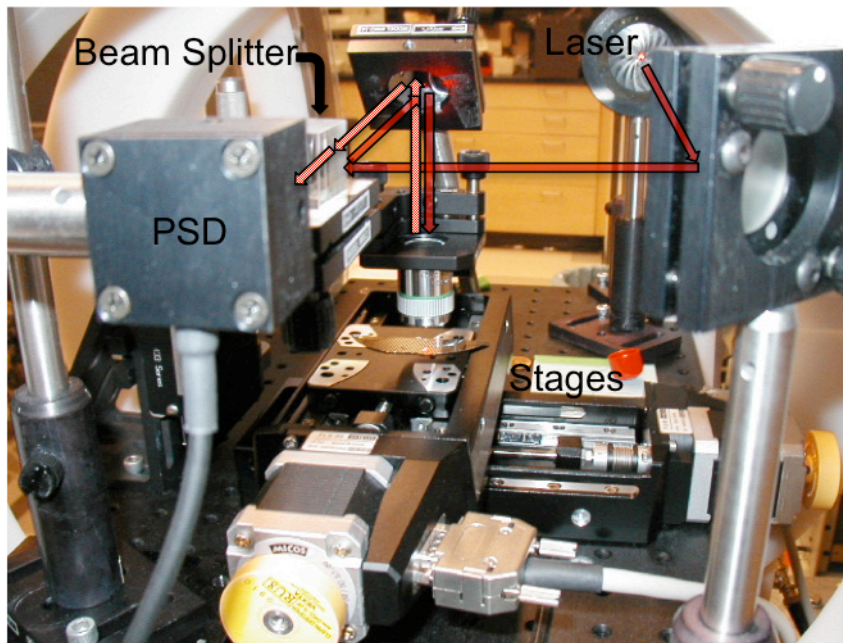
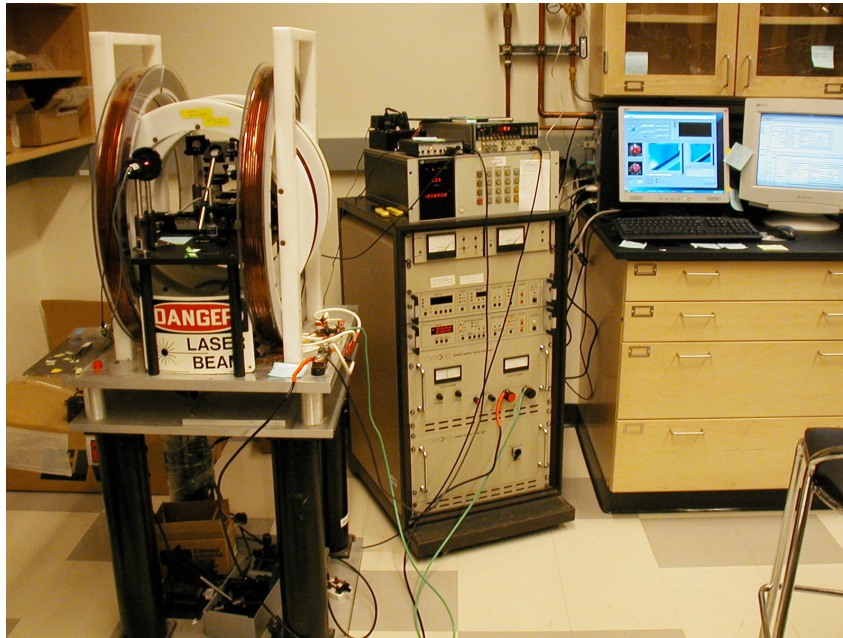


Figure 2.8: (Top) Two sets of Helmholtz coils are set on top of air-table for vibration isolation. In the middle of the photograph is the power supply used for application of magnetic field in two orthogonal directions and on the right is the computer used for VCI data acquisition and stage movement. Placed inside the Helmholtz coils are the optical measurement setup and precision stages (below).

2.6.4 Integration of Precision Stage Movement & Scanning Algorithms

Two MICOS precision linear translational stages are mounted orthogonally on the optical bench such that they are aligned with the directions of the optical line-of-sight, which is also aligned with the directions of applied magnetic fields. LabView control program packaged as stage controller from the vendor is fully integrated into the VCI at the machine-level programming. Using a serial bus interface, the VCI is programmed to control the stages to do a variety of tasks including scanning along a specific direction and/or in a grid. The resolution of the stage enables precise alignment with respect to the position and orientation of tip of the cantilevers. Cantilever array samples are placed onto the translational stages such that the orientations of the cantilevers are approximately parallel or perpendicular to the magnetic fields. Then, the alignment registration and calibration are subsequently implemented in the VCI program as an additional layer of precision.

Each MICOS translational stage communicates with the VCI LabView program via RS-232 using the serial port attached to the computer. Earlier attempts at controlling the stage movements utilized direct read and write commands through included sub VI program from MICOS (Fig 2.9 top). Due to the unreliability in communication, a checking routine was implemented after every command for the stage movement command to ensure that the stage position was identical to the desired stage position (Fig 2.9 bottom). As the program evolved, position tracking and error-checking necessitated constant communication with the translational stages (Fig 2.10). By incorporating stage control commands into a separate loop, it became possible to simultaneously execute and monitor stage movements while performing other program functions such as application of magnetic field for magnetostriction measurements.

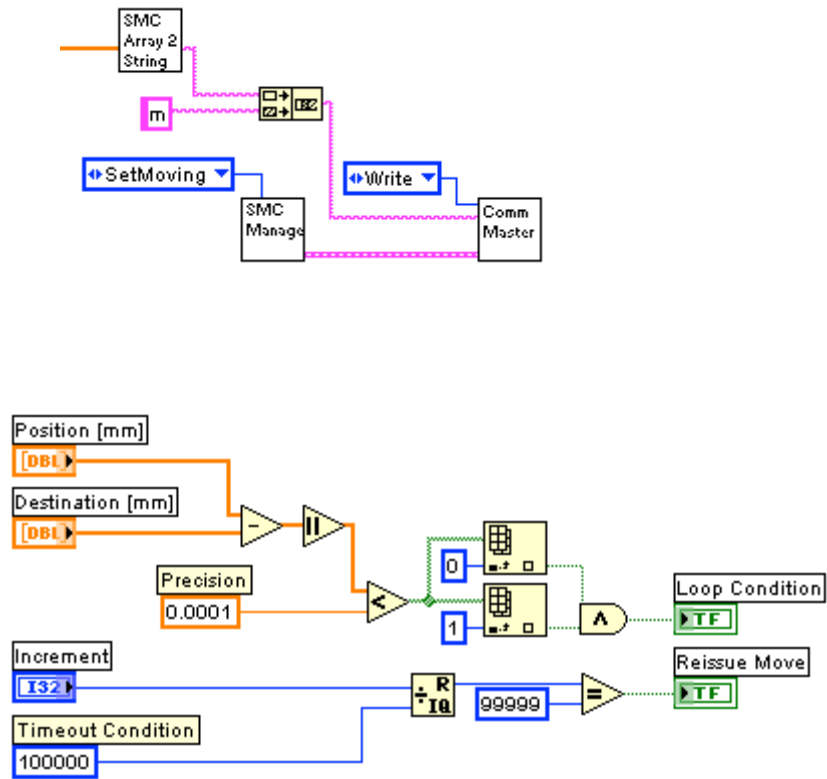


Figure 2.9: (Top) A portion of the VCI LabView diagram showing stage communication with array movement, and (bottom) the sub algorithm that ensures positional accuracy of the MICOS translational stages.

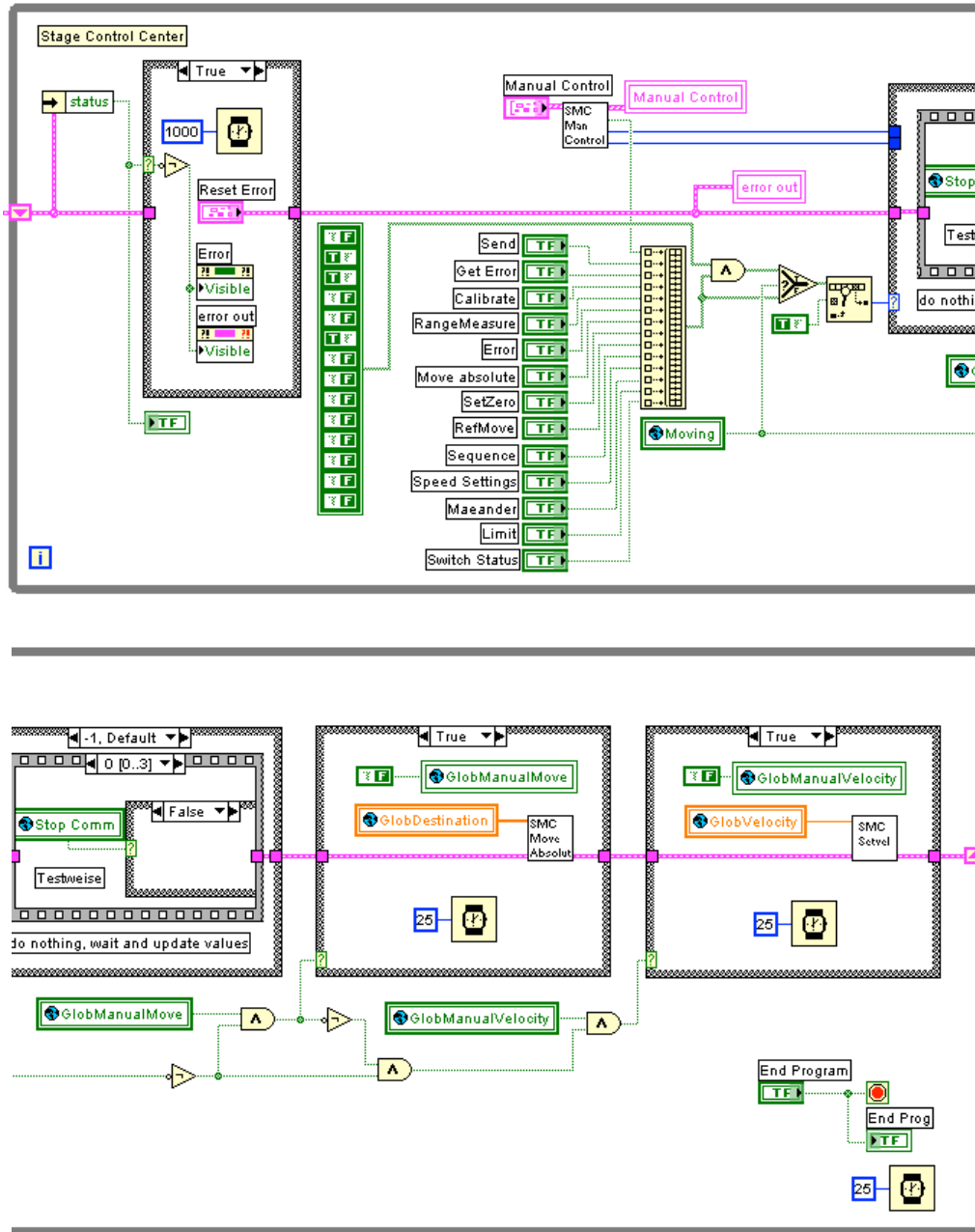


Figure 2.10: The LabView algorithm that constantly queries the stages, checks for errors and initiates commands. Predetermined stage movements in array measurements as well as manual movements can be executed. Simultaneous execution and monitoring of stage movement allows functions such as magnetization to be integrated in the VCI.

2.6.4.1 Calibration to Wafer Rotations

There is no physical mechanism used to align wafers on the stage such that the length of the cantilevers is along the axes of translational stage movements (and along the magnetization directions). It is therefore necessary for the software to account for small wafer rotations that might occur during sample mounting. Since the cantilever array is fabricated by photolithography, the position of any cantilever in the array can be precisely located after reference points have been identified. The calibration feature that has been chosen is the middle of the base of a cantilever.

Calibration points can be determined within an accuracy of approximately $5\ \mu\text{m}$ (MICOS stages have resolution of $1\ \mu\text{m}$). In order to improve accuracy, three reference points are used to define the rotation of the wafer (Fig 2.11). The original calibration algorithm used two reference points to determine an angle of rotation to calculate cantilever positions. In practice, this method proved to be less accurate than using two distinct translation vectors (Fig 2.12 top). Movement based on the calibration vectors has reliably allowed for precise sample positioning (Fig 2.12 bottom).

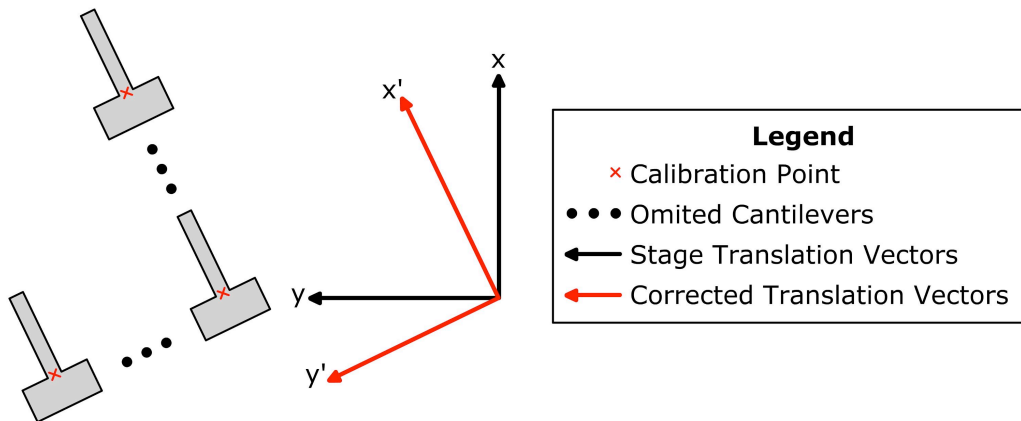


Figure 2.11: An illustration of the locations of the calibration points on the cantilever array, and how translation vectors for the stage movement are created.

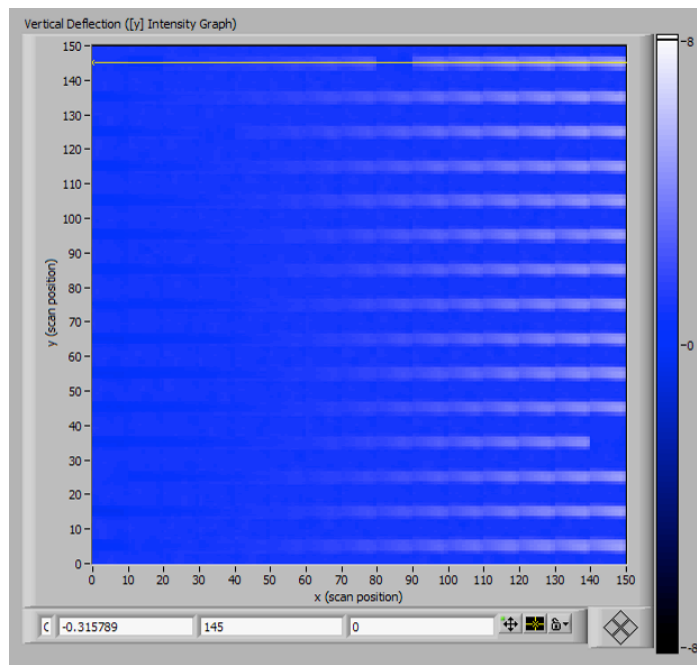
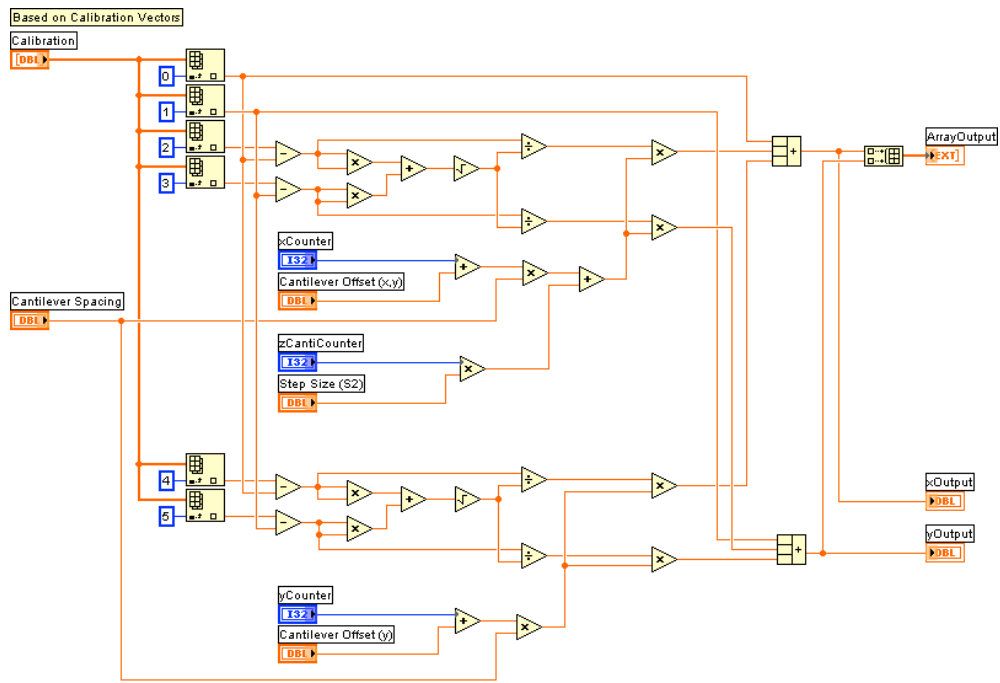


Figure 2.12: (Top) The LabView movement algorithm that accounts for wafer rotation, and (bottom) the scan of an array of cantilevers that demonstrates positional accuracy. The measurement scans a 10x10 grid surrounding a desired point on a cantilever, and then moves to the next cantilever in the array. After alignment calibration the scanned 15x15 cantilever array is arranged as they are physically on the wafer. The axes show the number of data points acquired.

2.6.4.2 Scanning Algorithms

The LabView program `arrayscan.vi` is used to determine intrinsic stress (Fig 2.13 left). It scans many points along the cantilever in order to better calculate cantilever curvature. A reference point is taken off of the cantilever to account for any wafer curvatures. the program scans all cantilevers in a specified region. `Magarrayscan.vi` is a fast algorithm designed for for magnetostriction and magnetostrictive susceptibility measurements (Fig 2.13 middle). It first changes the magnetic field to a specified value through the power supply. While holding the magnetic field constant, it then initiates `arrayscan.vi`. The process is repeated for various incremental magnetic fields. However, the lack of data point averaging and the small number of data points decrease the accuracy of measurements using this algorithm. `Arraymagscan.vi` is slow algorithm for magnetostriction and magnetostrictive susceptibility (Fig 2.13 right). This sub `vi` routine first finds a cantilever, and then ramps the magnetic field to its maximum value and back down. The scan continually takes readings of a specific point on the cantilever and a reference point off of the cantilever. The process is repeated for every cantilever in a specified region. This is much more accurate than `magarrayscan.vi` due to the large number of data points acquired, but much slower.

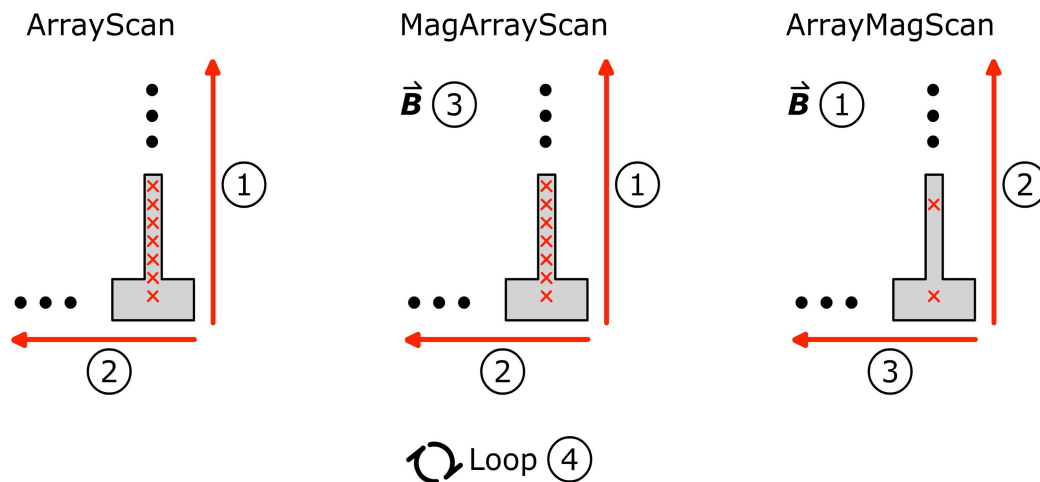


Figure 2.13: Schematics of the three primary scanning algorithms. Circled numbers indicate the priority order of movement commands.

2.6.4.3 Scanning Efficiency

Reducing the time required for scanning is important to achieve high-throughput measurements. Currently, the fastest magnetostriction measurements for complete ternary spreads are estimated to take 4 hours while the longest are estimated to take 4 days. The three most time-consuming processes are power supply ramping, stage movements and data acquisition that take minutes, seconds and tens of milliseconds respectively. The algorithm in `magarrayscan.vi` attempts to reduce the number of power supply ramps. However, preliminary measurements using this algorithm reveal poor trends (low precision and accuracy) due to the small number of data points taken. It is also possible that sustaining magnetic fields for long periods of time may lead to heating problems and variations in the data. The most promising solution would be to use a power supply that has much faster ramp rates. Stage movements already occur at a relatively fast velocity. Thus, time can only be reduced by decreasing the distance traveled. The current algorithm executes grid-based scans in a saw-like pattern, as these provide the shortest distances (Fig 2.14).

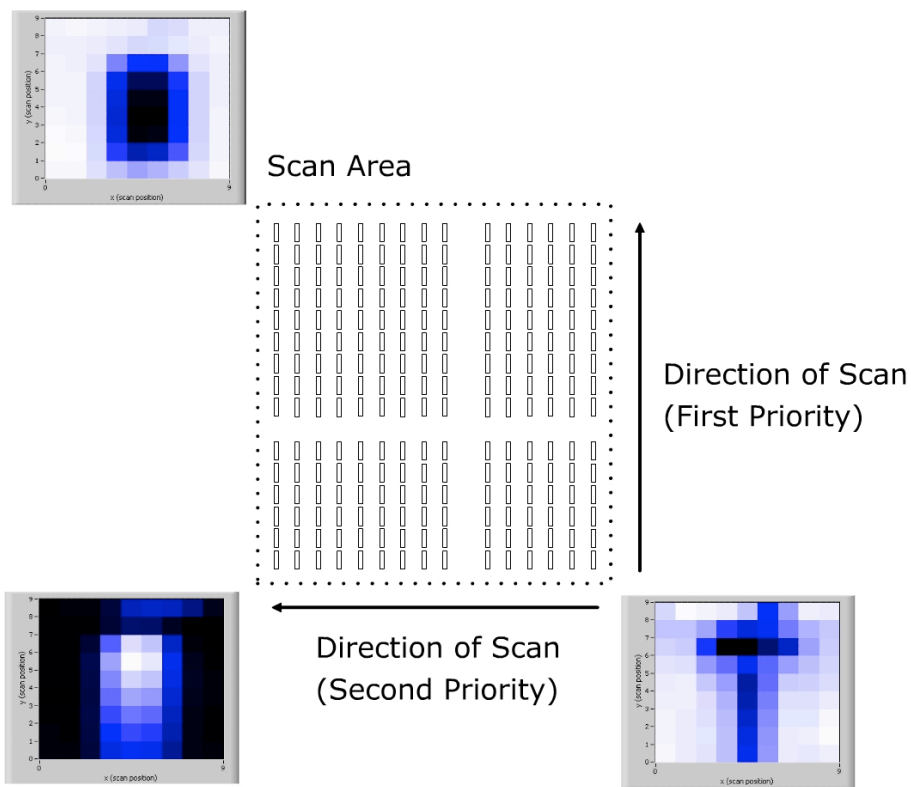
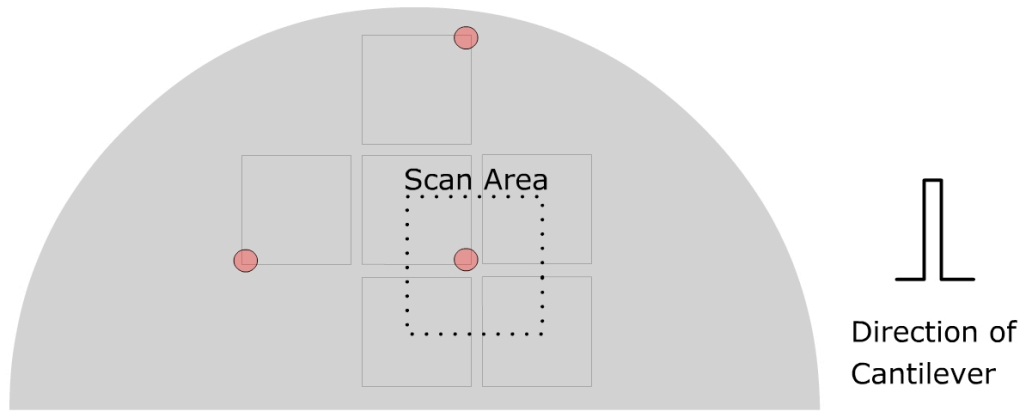


Figure 2.14: Scanning routine for the array describing the first priority along the length of the cantilever and the second as latitudinal. The stage movement is programmed to scan the length of a cantilever, then moved along the same direction on to the next cantilever. Once the column is finished scanning, stage is moved to the adjacent column of cantilevers and raster along that column while PSD signal is acquired continuously.

There is significant time spent to stop and start the stage in order to properly correlate stage positions with PSD measurements. Tests have been performed with algorithms that attempt data collection without stopping stage movements. However, even at slow velocities, acquired data indicates lost resolution as readings appear to be smoothed over position. One way to reduce the PSD data acquisition time is by decreasing the amount of data points collected. For example, only one PSD channel needs to be queried to measure cantilever deflections as they occur only in a single direction. In scans such as Magarrayscan.vi, holding the current source constant only requires magnetic field readings to be queried occasionally. The laser spot is another concern. Due to the static nature of the optical measurements, the spot size must be smaller than the cantilever in order to accurately quantify deflections. This system uses a pinhole aperture and objective lens to reduce the laser spot size to an estimated width of 10 μm when focused. However, the uncollimated light from the lens cannot accurately measure features far off of its focal plane. Moving above or below the focal plane will cause an increase in the spot size, which can cause unpredictable PSD measurements and light scattering. This may become significant when samples with high magnetostriction cause cantilevers to deflect significantly. Trials in which additional lenses were added or in which the light was collimated into a smaller beam were largely unsuccessful due to the limited space within the optical bench. One promising solution is to take measurements closer to the cantilever base, but is expected to reduce the sensitivity of the measurement.

CHAPTER 3

RESIDUAL STRESS MEASUREMENTS
IN
THIN FILM COMPOSITION SPREADS

3.1 INTRODUCTION

Residual stress measurements of composition spread samples were carried out to demonstrate the capabilities and efficiency of the high-throughput measurement system. In this chapter I describe in detail the operation of the measurement system.

3.2 EXPERIMENTAL DETAILS

Although there have been many advances in experimental tools for measuring curvature, the underlying principle for the analysis of the stress is the Stoney formula, as originally derived in 1909 [38]. This well-known formula relates the curvature of the film-substrate system to the differential stress between the film and the substrate. The stress σ was inferred from the radius of curvature ρ using the relationship

$$\sigma = \frac{E_s t_s^2}{6 t_f (1 - \nu_s)} \frac{1}{\rho}$$

where E_s is the elastic modulus of the substrate, t_s is the substrate thickness, ν_s is the Poisson ratio of the substrate, and t_f is the thickness of the film. All the parameters were known except for E_s which was determined using nanoindentation. Our setup used singly-clamped cantilevers as substrates with thin film deposits. The resulting curvature was detected using an optical laser/position sensitive detector (PSD) system. A set of precision linear motorized stages were utilized for cantilever maneuvering and were controlled by the VCI via serial bus interface.

3.2.1 Sample Production for Residual Stress Measurements

The silicon nitride substrate platform used in combinatorial measurement was produced by MEMS fabrication techniques. The entire micro-fabrication process is described in detail in Chapter 2. Reproducibility of the silicon nitride substrates greatly improved automation of high-throughput measurements. Because batch processing was carried out to produce multiple substrates simultaneously, discrepancy between individual cantilevers either from the same substrate or within the same batch was at a minimum. As a result, measurement uncertainty common to one-off experiments is almost negligible in our high-throughput measurements.

Deposition of thin film composition spreads was carried out by co-sputtering of multiple elemental sources. The details involved in co-deposition of pre-fabricated substrates are discussed in Chapter 2. When a pre-fabricated substrate containing silicon nitride cantilever array was deposited with a ternary film, each cantilever in the array was coated with unique composition. Therefore each cantilever was expected to exhibit distinct stress corresponding to its composition. To measure composition dependent intrinsic stress, Fe-Ni-Al ternary spreads were deposited. In particular a film containing 1:1:1 composition ratio of Fe:Ni:Al at the center of the substrate was prepared to demonstrate combinatorial residual stress measurement.

Two Fe-Ni-Al films were deposited using identical deposition conditions. One film was deposited on a bare silicon wafer and the other on pre-fabricated wafer containing a cantilever array. These two films were expected to have identical composition makeup as a function of position [40]. The coated cantilever array was used to map the residual stress of the composition spread. The unpatterned (blanket) film on the bare silicon wafer was used for composition analysis with EDX and for nanoindentation measurement to determine elastic modulus as a function of composition.

3.2.2 Experimental Setup for Residual Stress Measurements

The top row in figure 3.1 shows the images of an individual cantilever obtained to verify the optical measurement system. The figures were plotted using PSD voltage signal versus position by moving the sample in a square grid scan. When the cantilever and substrate were at the same angle of inclination, the PSD voltage was measured to be constant as expected (Fig 3.1 top row). The approximately 45° angle of the $\langle 111 \rangle$ silicon plane from KOH etching deflected the light off the PSD and the voltage reading became highly negative. The sharp PSD reading changed at changes of inclination were indicative of a well-focused laser on the cantilever. The resolution of the apparatus was sufficient to identify the fine texture at the bottom of the cantilever pit, even though the pit is displaced significantly from the focal plane. There are two potential explanations for the contrast observed near the tip of the cantilever: (1) the tip curvature may be so large that it causes the reflection to fall off the PSD, or (2) the scattering of light from edges and walls of the pit, distorting the spot of light that falls on the PSD. The latter would be a consequence of beam widening when the beam falls on features lower than the focal plane. Also, the light may reflect off of the bottom of the cantilever and cause an unpredictable scattering of light. Therefore, we concluded that it was important to ensure that line scans were along the middle of the cantilever and far enough from the tip to prevent erroneous readings. The bottom left of figure 3.1 presents an optical micrograph of an array of cantilevers used in the residual stress measurement. The precisely known location of each cantilever in the array was critical in achieving automation of stress measurements. Note that all the cantilevers seen in the micrograph have similar small angles of declination, representing the similar levels of low compressive stress present in the film. The small curvature associated with low compressive stress did not pose much challenge in the measurement and optimum sensitivity could be achieved. However highly curved cantilevers, as shown in figure 3.1 bottom right, imposed difficulty in this measurement. If the tip of the cantilevers were to use in stress determination, the PSD voltage corresponding to the high angle would go off the detector – i.e., would be reported as zero voltage. In this scenario, measuring the angle of inclination closer to the base of the

cantilever would allow determination of the stress although it would be at an expense of sensitivity. A reasonable approach therefore would be to measure the distance from the base that it took to achieve a given small declination (or the value of the declination at the tip). If that value were less than the target value, this would ensure that the measurement was always taken in the small declination limit.

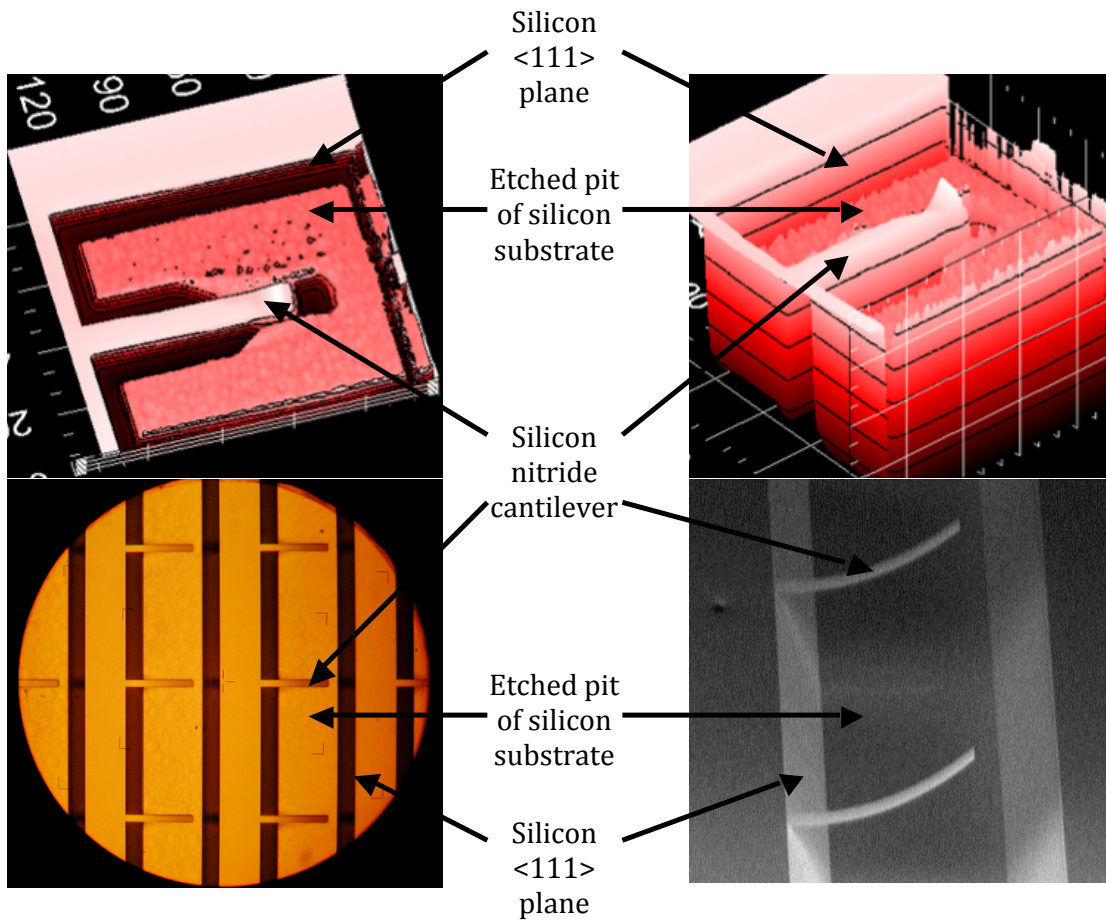


Figure 3.1: (Top row) 3D representations of an area scan of an individual 750um cantilever. The bumpy topography in the pit (pink region) illustrates high resolution of the measurement system. (Bottom left) A small subset of an array of cantilevers (500umx50umx1um); they are located on 1mm centers in both x and y directions. (Bottom right) A scanning electron micrograph of the same cantilevers under significant residual stress from sputter deposition is shown.

3.3 RESIDUAL STRESS MEASUREMENT & ANALYSIS

The angular deflection of the laser beam was measured in both **x** and **y** directions of the cantilever using the PSD. In this experiment the only relevant direction was the deflection along the long cantilever axis. The relation between PSD signal and angular deflection was calibrated using a mirror carefully elevated on the stage so that the focal plane of focused laser beam from the microscope objective was at the same level as that of a cantilever. The distance between the objective lens and the sample was compensated to correct for any significant changes in the focal plane, which otherwise would smear out the signal. The angle of the mirror was systematically varied and the corresponding PSD voltage measured. This calibration step was essential for reliable quantitative measurements.

Figure 3.2 top shows a calibration plot of the PSD voltage versus elevation angle of a mirror, confirming a linear relation with a slope of 2.1 V/degree. This calibration procedure was repeated several times and averaged to obtain the mean value which was to be used in scaling of the PSD voltage readout corresponding to the angular deflection (Fig 3.2 bottom). The uncertainty of the calibration factor was less than 5%. Once the calibration factor was determined, we could calculate the angular deflection θ at the end of the each cantilever using the relationship,

$$\theta = \text{PSDvoltage} \times 2.1 \text{ voltage/degree}$$

Ideally the curvature of the bent cantilever could be determined by plotting the PSD voltage as a function of distance from the fixed end, a straight line would be obtained whose slope would be the radius of curvature, ρ , of the cantilever. However not all data points taken along the cantilever should be used in calculation. Because it is possible to have huge curvatures in composition spreads, large angles of deflection may not be detected by the PSD and instead, any light present would be recorded as the corresponding value. This could lead to erroneous determination of curvature and thus must be resolved. A new approach involving a small angle approximation is attempted.

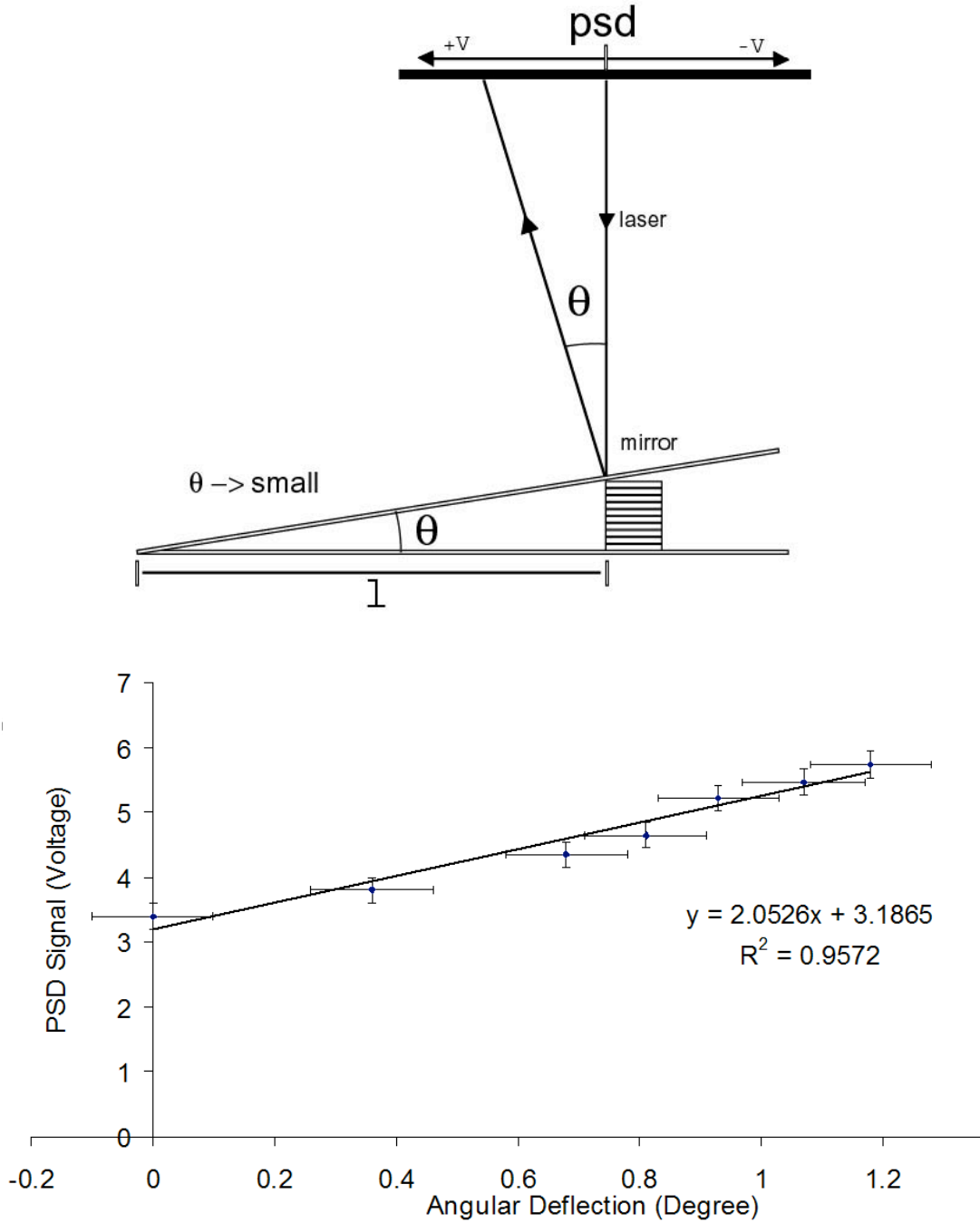


Figure 3.2: (Top) A schematic of calibration for small angles with voltage change in PSD. (Bottom) The calibration factor is the slope of the PSD voltage versus Angular deflection θ .

Regardless of the size of deflection, any radius of curvature should have significantly small angle of inclination closest to the fixed base of the cantilever because the fixed base was connected to the substrate (angle of inclination is zero). Therefore only the first few data points along the cantilever were required to determine the bending curvature of the cantilever.

Since the film thicknesses could be as large as 500 nm and the thickness of the substrate was only 1 μm , the approximations used to derive the Stoney formula were no longer strictly valid. Instead, a more general formula, derived in [41], must be used. This formula is valid over the whole range of film/substrate thickness ratios:

$$\sigma = \frac{E_s t_s^2}{6 t_f (1 - \nu_s)} \frac{1}{\rho} \Gamma$$

$$\Gamma = \frac{1 + \eta}{1 + 4\alpha\eta + 6\alpha\eta^2 + 4\alpha\eta^3 + \alpha^2\eta^4}$$

$$\alpha = \frac{E_f}{E_s}; \eta = \frac{t_f}{t_s}$$

where :

- ρ = radius of curvature
- E_f = Young's modulus of film
- E_s = Young's modulus of substrate
- t_f = thickness of film
- t_s = thickness of substrate
- ν_s = Poisson ratio of substrate

where ρ is the radius of curvature, E_f is Young's modulus of the film, E_s is Young's modulus of the substrate, t_f is the thickness of the film, t_s is the thickness of the substrate, and ν_s is Poisson's ratio for the substrate. The extra factor, Γ is included to account for the ratios between film and substrate' elastic moduli and thicknesses.

Required elastic moduli values were obtained from nanoindentation measurements using the other Fe-Ni-Al film coated on bare silicon wafer. Using a triangular Berkovich indenter, modulus data were taken at 10 mm interval covering the same 50 mm x 50 mm region of the film coated on the 2,500 cantilevers used in the stress measurement. Intensity plot (Fig 3.3) showed that the difference of elastic moduli among the various compositions is within the resolution of the nanoindenter used (10%); and therefore elastic moduli for the entire Fe-Ni-Al film may be taken as constant at the average value of 145 GPa.

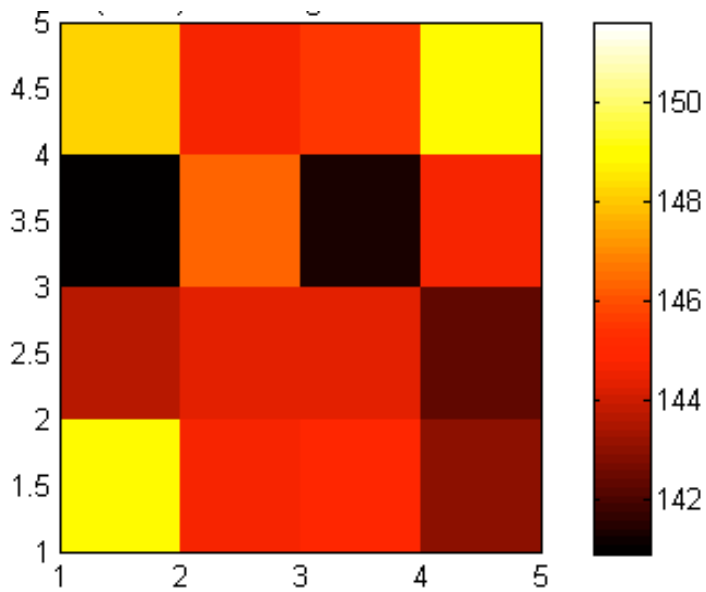


Figure 3.3: Intensity plot of elastic moduli of compositions in the middle 2,500 mm² region of Fe-Ni-Al film. The column on the right is the intensity scale in GPa.

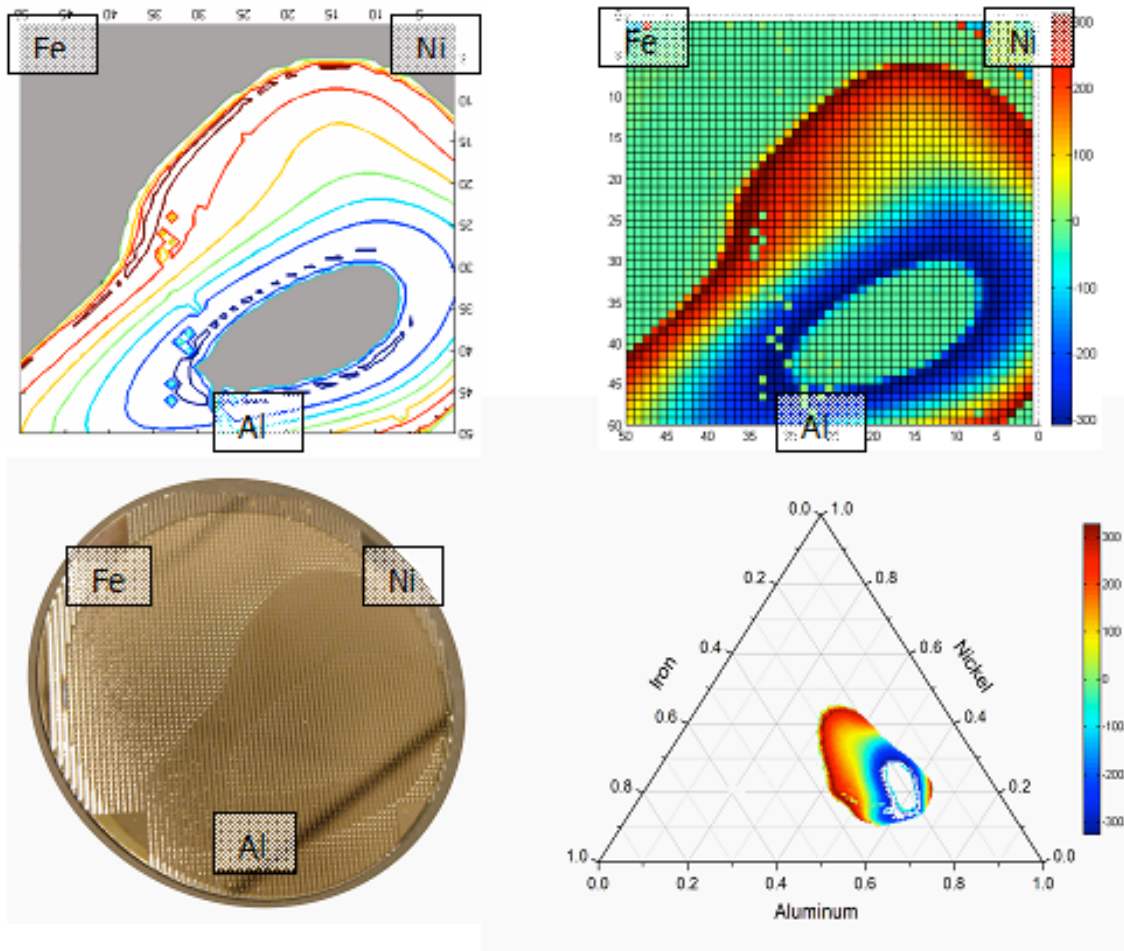


Figure 3.4: (Top left) Contour map of residual stress in Fe-Ni-Al films deposited in our system, as determined by cantilever deflections. (Top right) Same data plotted using a color map. (Bottom left) Image of Fe-Ni-Al composition sample on a 3-inch wafer with prefabricated cantilever array. Labels indicate the approximate position of the elemental sources creating the composition spread. The dark line is an artifact introduced by the photographic equipment. (Bottom right) Ternary phase diagram of the system showing composition dependent residual stress is plotted.

The data analysis is rapid using a MatLab script and typically takes a few minutes. The measurement of residual stress yields a single number for each cantilever. These values are plotted for a Fe-Ni-Al composition spread at the x, y positions of cantilevers in figure 3.4 top row. The pattern of stresses can be qualitatively observed by visual inspection of the wafer, as witnessed by the photograph (Fig 3.4 bottom left). The x and y axes represent the cantilever index as well as physical dimensions since the cantilevers are located on exact 1 mm centers. The dark gray areas in the contour plot and green areas in the surface plot indicate the deflections of cantilevers (tensile or compressive) that are so large as to drive the reflected beam off the PSD sensing area. This limits the dynamic range of the measurement with the present optical configuration to +/-300 MPa corresponding to minimum bending radius of approximately +/- 0.7 millimeter. It is straightforward to increase the dynamic range by adjusting the positions of the optical elements, although this will incur a penalty in minimum detectible stress resolution. The range of our system covers radii of curvature from roughly 0.7 millimeter to about 1 meter. The S/N ratio of the system is approximately 3×10^3 (70 dB). The lower right panel of figure 3.4 shows the same data mapped onto a ternary composition diagram using EDX composition data obtained at 25 points, which is then interpolated.

3.4 DISCUSSION OF EXPERIMENTAL ARTIFACTS

3.4.1 Optical Measurement Setup

The 5-mW diode laser used in the residual stress experiment has an elliptical beam spot and focusing was extremely difficult. Collimating the beam was impossible due to its shape and divergence, although small, was not controllable. Its intensity was a problematic issue because the bright beam scatters off the surrounding to give off confusing signal in the PSD. Therefore the laser was modulated to operate at less than 30% duty cycle to reduce its luminosity. This reduction also helped alleviate the heating of the cantilever which was an important concern dealing with metallic thin films. Thermal expansion of metal film on non-metal substrate would certainly influence the measurement. To mitigate this problem, optimized algorithms were used to reduce the amount of time the laser hits the cantilevers. The high thermal conductivity and highly reflective surfaces of metal further reduce the heating.

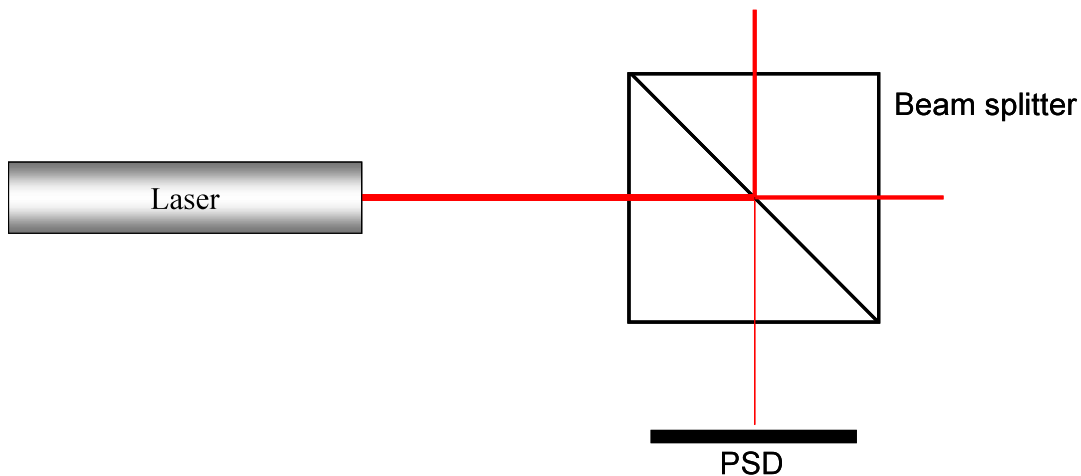


Figure 3.5: Unwanted reflection of laser light from the beam splitter leads to systematic error and undesired reduction in measurement sensitivity.

The 50% beam splitter and the PSD used in the experiment were not ideal instruments. The beam splitter contributed to light contamination during measurement due to an internal interface which produced an additional dim laser spot (Fig 3.5). This laser spot was always

present in the measurement and contributed to systematic error. The PSD was designed to find the centroid of the light detected on its surface and an extra light spot creates an error artifact. Part of the light incident on the PSD was reflected back to the substrate. When measuring areas of small deflection, the reflections between the PSD and the substrate yielded as many as three distinct laser spots. An ideal PSD would have a large sensing area such that moving it farther away from the sample to improve measurement sensitivity would not sacrifice the range in measurements. This was not the case with the 4mm x 4mm detecting surface of the PSD currently employed. This was too small to be fixed in one position, as would be otherwise possible with a larger PSD. The PSD was positioned close to the sample in the measurement setup in order to detect a wide range of deflections.

Other sources of light contamination include ambient light in the room. Large black plastic bags were used as a light shield covering the apparatus, but these did not completely eliminate the stray light. Trials performed in the presence of external lights were observed to dramatically skew PSD measurements, creating a wavy pattern as shown in figure 3.6.

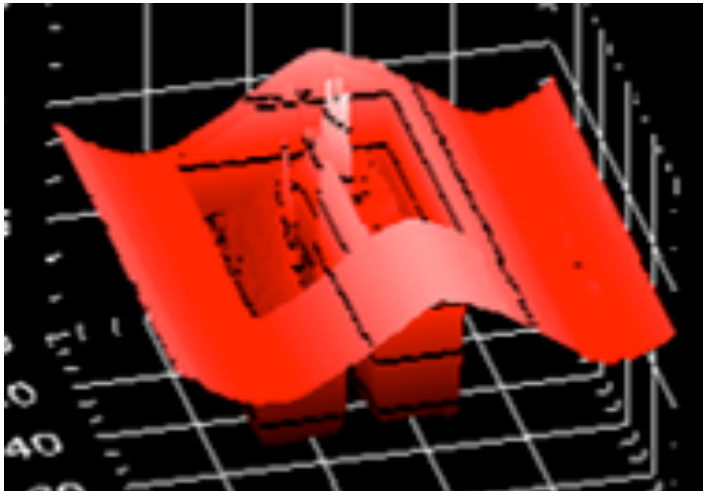


Figure 3.6: Wavy pattern observed in the 3D scan is due to the stray light mainly coming from the ceiling light bulbs that are flickering at 60 Hz.

3.4.2 Stability of Measurements for The Entire Cantilever Array

A typical experiment, in which 2500 cantilevers were measured, took approximately 2 hours. Measurements of PSD signal drift allowed us to conclude that the drift was negligible over a time period of 2 hours, far longer than the time needed to measure a single cantilever (Fig 3.7).

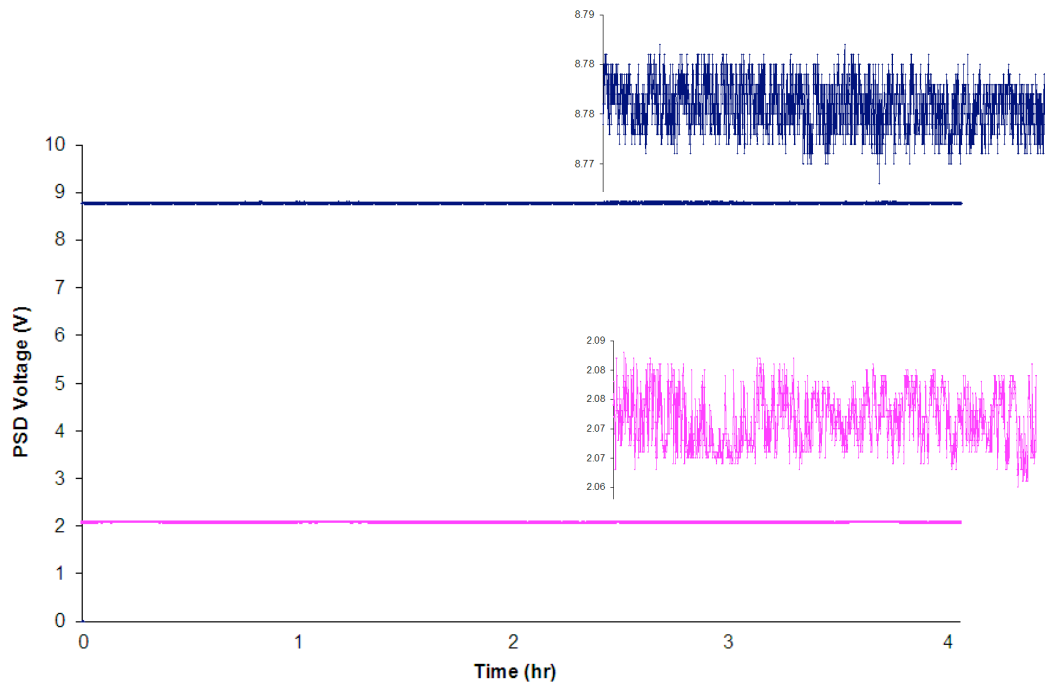


Figure 3.7: Plot of drift test over a 4-hour period: data set in blue is obtained from the x-direction and red is from y-direction of the PSD readout. Small fluctuations in the PSD voltage as acquired through the data acquisition system can be seen in the insets above each data set, and are attributed to environmental vibrations coupled to the apparatus.

3.4.3 Influence of Environment

Thermal expansion may occur due to environmental temperature changes surrounding samples during testing. Sources include heat emanating from the laser and Helmholtz coils, and local changes of temperature in the room. Ambient stray light on the detector also influenced measurements and hence the entire experiment assembly has to be covered to ensure stray light does not enter during the measurements.

CHAPTER 4
MAGNETOSTRICTION MEASUREMENT

4.1 INTRODUCTION

Magnetostriction is a basic property of ferromagnetic materials which exhibit a fractional change in physical dimensions under an applied magnetic field. Length and/or volume magnetostriction occur by changing orientation of its magnetic moment with respect to its crystal lattice. It is a small effect on the order of tens of parts per million (ppm). While measurement of magnetostriction in bulk materials is readily accomplished using a strain gauge for the bulk samples, measurement of this quantity for thin films presents a greater challenge, and typically involves measurement of the overall wafer curvature (for a film of uniform composition) as a function of the magnetic field. MEMS tools for high-throughput characterization were first described by the Takeuchi group [13,21] in the context of qualitative measurements of shape-memory alloys, while individual cantilevers have long been used for the quantitative study of thin film properties. In order to evaluate magnetostriction locally in composition-spread samples, the best suitable method is to combine and extend these approaches to make a MEMS platform that can yield quantitative, reliable measurement of mechanical properties as a function of composition. A significant complication is the requirement that the dimensions of the cantilever be small enough to ensure that the composition of the film being measured does not vary. Therefore this investigative technique was developed to utilize a dense array of pre-fabricated MEMS cantilever beams similar to the residual stress measurement setup in Chapter 3. The differential strain in the thin film/cantilever system due to magnetostriction resulted in curvature change that can be detected using an optical (laser/position-sensitive-detector) system, also similar to the residual stress measurement setup. A magnetic field was applied using two orthogonal Helmholtz coils, and the resulting deflection-field curves were used to determine the saturation magnetostriction λ_s as well as magnetostrictive susceptibility $d\lambda/dH$. The composition-spread films were prepared using a three-gun on-axis DC magnetron co-sputtering system as shown in Chapter 2. The position-dependent composition was inferred using rate calibrations and verified with electron microprobe. Preliminary residual stress experiments from Chapter 3 had validated the technique and this system had been used to measure magnetostriction in the Ni-Fe

system. Small cantilevers and a highly sensitive optical measurement system allow this system to explore large composition ranges at small composition intervals (approximately 1 atomic percent change per cantilever), as well as enable magnetostriction measurements with a resolution of approximately 1 ppm.

Table 1. Techniques for measuring magnetostriction in thin films.

Techniques	B-H loop tracer (indirect)	Capacitance (direct)	Optical- resonant (indirect)	Optical- nonresonant (direct)
Detection sensitivity	1 ppm	1 ppm	10 ⁻⁶ ppm	10 ⁻⁴ ppm

There are a number of different ways to measure thin film magnetostriction coefficient λ [3], as listed in Table 1. This coefficient can be indirectly inferred by measuring the anisotropy field of a given film-substrate system as a function of stress, using a B-H loop tracer or permeameter. This technique does not lend itself to high spatial resolution, and is most suited for measurement of uniform composition films, and has been widely used in the past. The magnetically induced deflection of a film/cantilever system is a particularly useful technique for quantitatively measuring the effect of magnetostriction; the deflection may be determined by either direct or indirect techniques. For direct measurements, some have used the capacitance technique in which the deposited film acts as a capacitor electrode while the detecting probe is used as the counter-electrode to form a complete capacitor, whose capacitance varies with the degree of film sample deflection [42]. Another way to measure the deflection is by using an optical technique, which has been the most precise method known to measure magnetostriction. One can resonantly oscillate a film-substrate cantilever and measure its resonant frequency shift in response to the applied magnetic field. Then the magnetostriction coefficient is indirectly but reliably extracted using this technique (the ΔE effect) [43]; however, the damping coefficient has to be carefully determined. Although not as sensitive as the resonant optical method, measuring the static deflection of a bent film-substrate system offers the direct measurement of the

coefficient of magnetostriction. This method requires a relatively simple experimental setup, also similar to the residual stress measurement setup from Chapter 3. In addition, sample preparation for this method is simpler and less expensive than for the capacitance technique. Hence this approach is adopted as the detection scheme for the high-throughput measurement of magnetostriction in the Ni-Fe system.

4.2 EXPERIMENTAL DETAILS

As in the residual stress measurements, determination of the radius of curvature of a cantilever was involved in this experiment. The radius of curvature of intrinsically strained cantilever was measured as a reference prior to applying the magnetic field. To determine the magnetostriction coefficient, a uniform magnetic field was then applied to induce magnetostrictive strain in the magnetic film deposited on the non-magnetic silicon nitride substrate. The stress-induced change in curvature was measured again. The difference between the changes in radius of curvature, hence deflection angles, was used to determine to magnetostriction coefficient for the particular magnetic composition. Measurements for composition spreads were automated by repeating individual cantilever measurements for the entire array which was positioned accurately. As described in Chapter 2, array measurement for the entire composition spread is facilitated through the use of integrated LabView program VCI.

4.2.1 Sample Preparation

As in the residual stress experiment, substrates containing MEMS-based silicon nitride Si_3N_4 micro-cantilevers were used. Magnetic thin films of thicknesses between 50 nm and 200 nm were deposited using a three-gun on-axis DC magnetron co-sputtering system and a stand-alone S-gun specifically for sputtering of magnetic materials. In particular, single composition films of $\text{Ni}_{60}\text{Fe}_{40}$ were deposited using the S-gun. Binary composition spreads of Ni-Fe were prepared to demonstrate the ability to analyze simple magnetostrictive trends. All films were deposited at different pressures and temperatures in order to determine conditions that yielded

minimal intrinsic stress, or samples that have cantilevers with the least deflection. Composition analyses were carried out using similar characterization techniques as described in Chapter 2 and 3.

4.2.2 Measurement Setup

The measurement setup was similar to the one used in residual stress measurements with the additional capability in the application of non-contact external magnetic field to the sample (Fig 4.1). These added components are the two sets of Helmholtz coils used for applying uniform magnetic field in orthogonal directions. Each pair of Helmholtz coils can generate up to ~100 Oe; they are powered by a single programmable power supply (Oxford Instruments, Oxford, United Kingdom) which can output a maximum of 25 Ampere to a single set of coils with a ramp rate up to 20 Ampere/minute. The power supply is controlled by the VCI through serial bus RS232 enabling automated current ramping; although switching the direction of applied current is only possible manually.

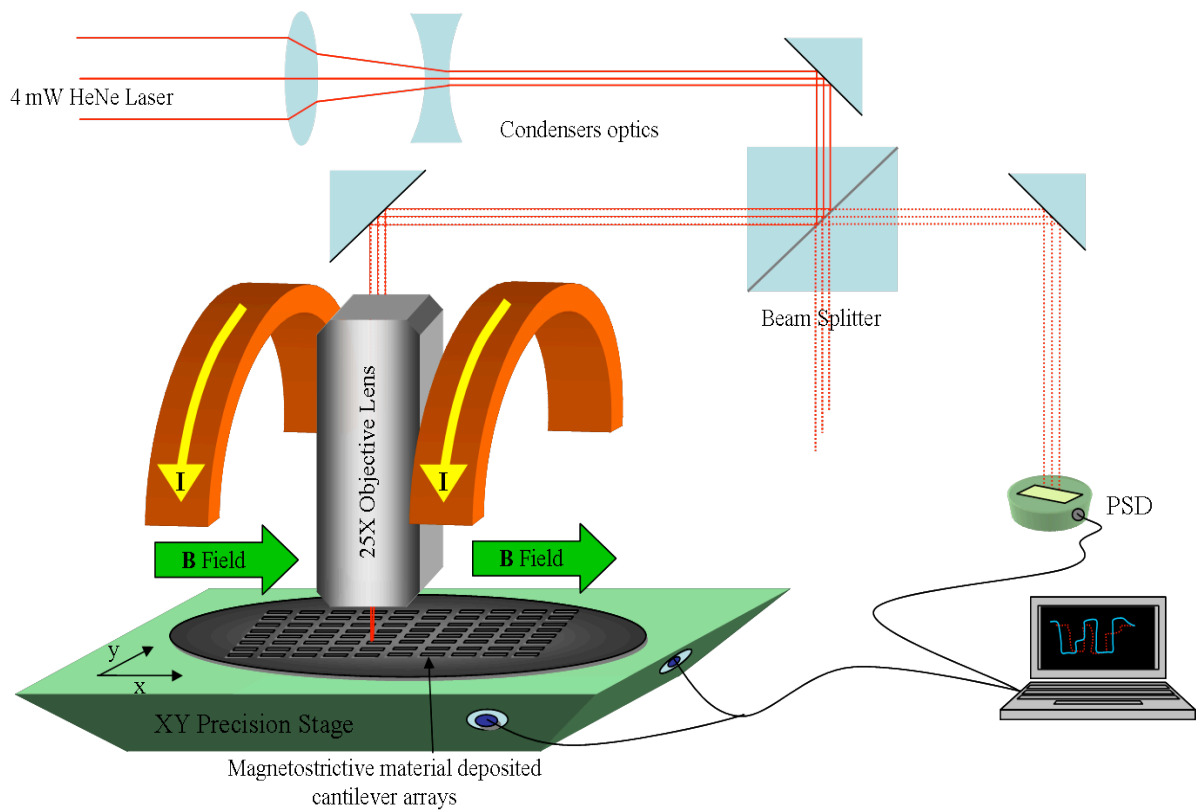


Figure 4.1: A schematic representation of the magnetostriction measurement system: two orthogonally placed translation stages are used. Orange-color arches represent a set of Helmholtz coils surrounding the optical measurement setup, including the stages.

4.3 CALCULATION OF MAGNETOSTRICTION

All the calibration procedures are identical to those used for residual stress measurement as described in Chapter 3. The average calibration factor was determined and used to scale the PSD voltage readout. With calibration factor of 2.1 V/degree, the deflection, D can be determined using the following relationship:

$$D = l \cdot \sin\left(\frac{\text{PSDvoltage}}{2 \text{ V/}^\circ}\right)$$

where l is the distance from which the measurement was taken, to the fixed base of the cantilever. Once the deflection value was obtained the magnetostriction coefficient was correlated to the deflection using a relationship by P. M. Marcus [44]:

$$\lambda = D \frac{E_s t_s^2}{E_f t_f 9l^2} \frac{(1 + \nu_f)}{(1 + \nu_s)(1 - \nu_s)} \quad [6]$$

where:

- λ = magnetostriction
- D = vertical deflection at end of cantilever
- E = Young's modulus
- t = thickness of film
- l = length of cantilever
- ν = Poisson ratio

The subscripts s and f are for substrate and film respectively. Using the known Poisson ratios $\nu_s = 0.24$ and $\nu_f = 0.30$ along with Young's moduli $E_{Fe} = 211$ GPa, $E_{Ni} = 200$ GPa and $E_{Si_3N_4}$ (LPCVD) = 290 GPa, the magnetostriction can be inferred directly from the angular deflection, which is proportional to the vertical deflection at the end of the cantilever, D. A Si_3N_4 cantilever that is 500 μm long and 1 μm thick cantilever substrate was coated with 100-nm film of $Ni_{60}Fe_{40}$, which has $\lambda_s = 20$ ppm. The vertical deflection at the end of the cantilever is therefore expected to be 2,175 nm.

$$\lambda = \left[\frac{l}{\sin\left(\Delta V_{PSD} \cdot \frac{Calibration^\circ}{V}\right)} \right] \frac{(290GPa)(1\mu m)^2}{\left(\frac{60}{100} 200GPa + \frac{40}{100} 211GPa\right)(400nm)^2} \frac{\left(1 + \left[\frac{60}{100} 0.31 + \frac{40}{100} 0.29\right]\right)}{(1 + 0.24)(1 - 0.24)}$$

$$= \frac{5.4449 \times 10^{-7} m}{l \sin\left(\Delta V_{PSD} \cdot \frac{Calibration^\circ}{V}\right)}$$

For the Ni₆₀Fe₄₀ film the measured value of λ is 14 ppm at 100 Oe, which is plausible since the magnetostriction has not actually saturated at this field strength (Fig 4.2 top). The root-mean-squared noise in the measurement is ± 0.6 ppm based on a Gaussian fit to the histogram of measurements (Fig 4.2 bottom). The slope of the plot of λ vs. field gives the magnetostrictive susceptibility, an important parameter of magnetostrictive actuators:

$$\frac{d\lambda}{dH} = 0.144 \text{ ppm/Oe}$$

that defines the magnetostrictive susceptibility (Fig 4.2 top).

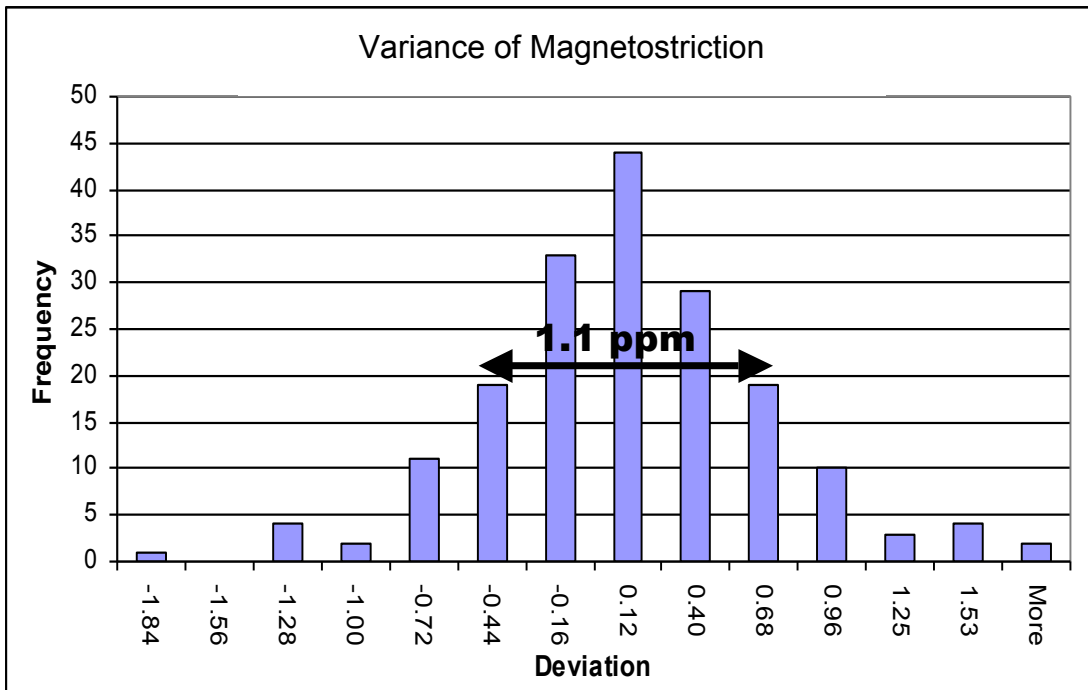
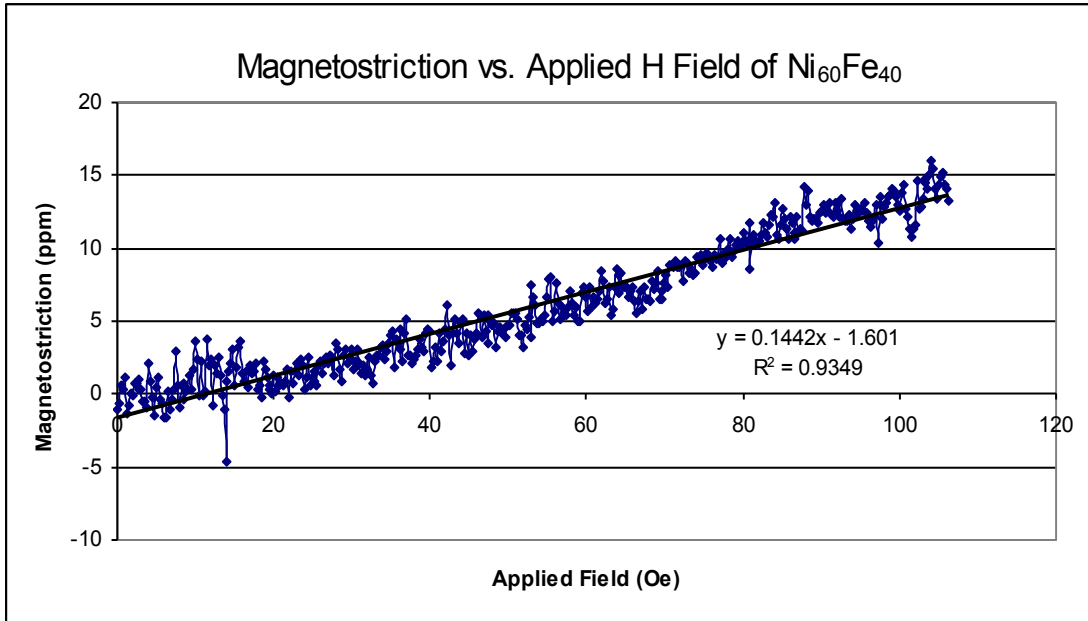


Figure 4.2: (Top) Plot of magnetostriction coefficient λ vs. applied magnetic field along the length of the cantilever for Ni₆₀Fe₄₀. (Bottom) λ , fluctuation levels on the PSD; FWHM of the Gaussian profile is 1.1 ppm.

4.4 RELIABILITY OF MAGNETOSTRICTION MEASUREMENT

After the first experiments on the $\text{Ni}_{60}\text{Fe}_{40}$ sample, the magnetostriction measurements described above could not be reproduced. Measurements of adjacent cantilevers during the first day did not show any changes in the PSD signal. Moreover, various magnetic samples were tested after the first day also failed to replicate the observed effect. At this point, measurements of the composition spread could not be made possible because the reliability of the measurement of a single cantilever could not be validated. After several days of attempts to test other samples, some of the measurements started showing a huge jump in the PSD signal as the magnetic field was applied. At some point, the jump in the signal could be observed even at a very low field, which suggested that the results were artifacts unrelated to magnetostriction. At this point, we suspected that something in the experimental setup was causing this behavior. To check, a mirror was used instead of the magnetic samples. Placing the laser spot on the mirror yielded the same jump in the PSD signal when the magnetic field was turned on. Carefully checking all the components in the experimental setup revealed that the leadscrews of MICOS translation stages had been indeed developed a permanent magnetic moment after many prolonged magnetization experiments. The leadscrews evidently had a history-dependent moment that could explain the jumps in the PSD signal as the Helmholtz coils were energized.

Although it might be possible to deconvolute this artifact from the observed deflections to obtain the true magnetostriction, at least for a single cantilever measurement, this effect of the leadscrews proved to be too unpredictable and too complicated to model due to the setup of the experimental components. When energized, the magnetic field inside the Helmholtz coils should contain a “sweet spot” of uniform magnetic field big enough to cover an entire 3-inch wafer. However when two MICOS stages, which were fastened orthogonally for movement in both x and y directions, moved to center the cantilever for the measurement, the stages themselves sometime went out of sweet spot, so the moment they contribute to the net field at the location of the cantilever would depend on the position of the cantilever along with the complete history of the measurement. Any nonuniformity in the field would also lead to a torque on the cantilever

with unpredictable magnitude. It is not clear whether it would be sufficient to predetermine the magnetic field at every x and y position on the 3-inch wafer. Depending on the exact position of the stages respect to each other, the magnitude of the signal jump might be adjusted according to the x and y coordinate of the stages. Preliminary attempts to incorporate effective compensation for the distortion of field due to the leadscrews were unsatisfactory; as a result it was concluded that the measurement system had an inherent flaw.

CHAPTER 5
CONCLUSIONS

5.1 SUMMARY & FUTURE PROSPECTS

A highly precise high-throughput measurement system for investigation of the mechanical properties of thin film composition spreads has been developed that offers unprecedented composition resolution. In this approach, thin film composition spreads are deposited on a dense array of MEMS-based prefabricated cantilevers. The curvature of the cantilevers is interrogated using an optical curvature measurement that is fast and precise. A LabView program is written to control the x-y stage is integrated with the data acquisition system to allow automated high-throughput measurements of local properties in composition spread samples. To demonstrate the capability of the measurement system, residual stresses were measured at 1 mm intervals on the Fe-Ni-Al composition spread film. Since the composition spreads typically have a composition gradient on the order of 1 atomic % per mm, this technique enables investigation of thin film stresses with 1 atomic % resolution. For a 3-inch wafer, it takes approximately 2 hours to measure 2,500 cantilever deflections, including the preparation time required for registration and alignment of cantilevers and calibration of detector sensitivity.

This measurement system has a relatively high dynamic range and high sensitivity, which can enable high-throughput investigation of a wide range of other mechanical properties, such as conventional and ferromagnetic shape-memory effects, thermal expansion coefficients, and magnetostrictive properties. To demonstrate the high sensitivity and versatility of this system, the thin film magnetostriction coefficient of Ni₆₀Fe₄₀ alloy was measured to be 14 ppm with the error in strain estimated to be as small as 0.1 ppm. Although additional LabView scanning algorithms were written to integrate magnetostriction measurement into the existing automation setup for local stress measurement, reproducibility of the magnetostriction measurement itself proved to be difficult, and unreliable even when adjustments due to the magnetic leadscrews are included. Future work should focus on ensuring the accuracy and reliability of measurements. The versatility of this measurement system will facilitate combinatorial investigations of functional materials properties, such as the recovery temperatures of shape-memory alloys.

BIBLIOGRAPHY

- 1] D.L. Smith, *Thin-Film Deposition: Principles and Practice*, McGraw-Hill, **1955**
- 2] L.B. Freund, S. Suresh, *Thin Film Materials*, Cambridge University Press, **2003**
- 3] A.C. Tam, H. Schroeder, *IEEE Trans. on Magnetics*, vol. 25, p 2629, **1989**
- 4] M. Nie, Q. Huang, W. Li, *Sensors and Actuators A* 126, p.93-97, **2006**
- 5] C. Taylor, D. Barlett, E. Chason, and J. Floro, *The Industrial Physics* 4, p.25, **1998**
- 6] A.J. Rosakis, R.P. Singh, Y. Tsuji, E. Kolawa, N.R. Moore, *Thin Solid Films* 325, p.42-54, **1998**
- 7] H. Lee, A.J. Rosakis, L.B. Freund, *Journal of Applied Physics* 89, p.6116-6129, **2001**
- 8] R. M. Bozorth, *Ferromagnetism*, Van Nostrand, Princeton, NJ, **1951**
- 9] E. Klokholm, *IEEE Transactions on Magnetics* 12, p.819-821, **1976**
- 10] E. Klokholm, C. V. Jahnes, *Journal of Magnetism and Magnetic Materials* 152, p.226-230, **1996**
- 11] A.E. Clark, J.B. Restorff, M. Wun-Fogle, T.A. Lograsso, D.L. Schlager, *IEEE Trans. Magn.* 36, p.3238–3240, **2000**
- 12] K.A. Ellis, R.B. van Dover, T.J. Klemmer, G.B. Alers, *Journal of Applied Physics* 87, p.6304-6306, **2000**
- 13] I. Takeuchi, O.O. Famodu, J.C. Read, M.A. Aronova, K.-S.Chang, C. Craciunescu, S.E. Lofland, M. Wuttig, F.C. Wellstood, L. Knauss, and A. Orozco, *Nature Materials* 2, **2003**
- 14] A. Ludwig, J. Cao, J. Brugger, I Takeuchi, *Meas. Sci. Technology* 16, **2005**
- 15] R.B. van Dover, L.F. Schneemeyer, R.M. Fleming, *Nature* 392, p.162–164, **1998**

- 16] R.B. van Dover, L.F. Schneemeyer, *Macromolecular Rapid Communications* 25, p.150-157, **2004**
- 17] Y. Muramatsu, T. Yamamoto, T. Hashimoto, T. Hayakawa, M. Yoshimoto, H. Koinuma, *Proceedings of the SPIE - The International Society for Optical Engineering*, Vol. 3941, p.92-99, **2000**
- 18] J. C. Meredith, A. Karim, E. J. Amis, *MRS Bulletin*, Vol. 27, p.330-335, **2002**
- 19] R. Hoogenboom, M.A.R. Meier, U.S. Schubert, *Mater. Res. Soc. Symposium Proceedings* 804, p.83-94, **2004**
- 20] A. Karim, K. Yurekli, C. Meredith, E. Amis, R. Krishnamoorti, *Polymer Engineering and Science* 42, p.1836, **2002**
- 21] O. O. Famodu, J. Hattrick-Simpers, M. Aronova, K. Chang, M. Murakami, M. Wuttig, T. Okazaki, Y. Furuya, L. A. Knauss, L. A. Bendersky, F. S. Biancaniello, I. Takeuchi, *Materials Transactions*, Vol. 45, p.173, **2004**
- 22] R. Hassdorf, J. Feydt, S. Thienhaus, R. Borowski, M. Boese, T. Walther, M. Moske, *Mater. Res. Soc. Symposium Proceedings* 785, p.57, **2004**
- 23] C.H. Olk, *Measurement Science & Technology* 16, p.14-20, **2005**
- 24] C.H. Olk, G.G. Tibbetts, D. Simon, J.J. Moleski, *Journal of Applied Physics* 94, p.720, **2003**
- 25] M. Prochaska, J. Jin, D. Rochefort, L. Zhuang, F. J. DiSalvo, R. B. v. Dover, and H. D. Abruña, *Review of Scientific Instruments* 77, 054104, **2006**
- 26] J. Jin, M. Prochaska, D. Rochefort, D.K. Kim, L. Zhuang, F.J. DiSalvo, R.B. van dover, H.D. Abruna, *Applied Surface Science* 254, p.653-661, **2007**
- 27] N.C. Woo, B. Ng, R.B. van Dover, *Review of Scientific Instruments* 78, 072208, **2007**
- 28] I. Takeuchi, R. B. van Dover, H. Koinuma, *MRS Bulletin* 27, p.301-308, **2002**
- 29] W.H. Lawson, *Journal of Scientific Instruments* 44, **1967**
- 30] I. Yanase, T. Ohtaki, M. Watanabe, *Solid State Ionics, Diffusion & Reactions* 154, p.419-424, **2002**

- 31] Y.S. Chu, A. Tkachuk, S. Vogt, P. Ilinski, D.A. Walko, D.C. Mancini, E.M. Dufresne, H. Liang, F. Tsui, *Applied Surface Science* 223, p.175, **2004**
- 32] D. Sander, H. Ibach, *Physical Review B* 43, p.4263-4267, **1991**
- 33] R. E. Martinez, W. M. Augustyniak, J. A. Golovchenko, *Physical Review Letters* 64, p.1035-1038, **1990**
- 34] P. Kury, P. Zahl, M. Horn-von Hoegen, *Review of Scientific Instruments* 75, p.2211-2212, **2004**
- 35] R. Koch, H. Leonhard, G. Thurner, R. Abermann, *Review of Scientific Instruments* 61, p.3859-3862, **1990**
- 36] M. Weber, R. Koch, K. H. Rieder, *Physical Review Letters* 73, p.1166-1169, **1994**
- 37] A. J. Schell-Sorokin, R. M. Tromp, *Physical Review Letters* 64, p.1039-1042, **1990**
- 38] G. G. Stoney, *Proc. R. Soc. London, Ser. A* 82, p.172, **1909**
- 39] On-Trak Photonics Corporation (<http://www.on-trak.com/2lseries.html>)
- 40] J.M. Gregoire, D. Dale, A. Kazimirov, F.J. DiSalvo, R.B. van Dover, *Journal of Vacuum Science & Technology A* 28, p.1279-80, **2010**
- 41] L. B. Freund, J. A. Floro, E. Chason, *Applied Physics Letters* 74, p.1987-1989, **1999**
- 42] M.S. Boley, W.C. Shin, D.K. Rigsbee, D.A. Franklin, *Journal of Applied Physics* **91**, p.10, **2002**
- 43] A. Ludwig, E. Quandt, *IEEE Transactions on Magnetics* 38, p. 2829-2831, **2002**
- 44] P. M. Marcus, *Physical Review B* **53**, p.5, **1996**